THESIS

PARSING PARP: THE ENZYMATIC AND BIOPHYSICAL CHARACTERIZATION OF POLY (ADP-RIBOSE) POLYMERASES I and II

Maggie RD Hepler

Department of Biochemistry & Molecular Biology

In partial fulfillment of the requirements

For the Degree of Master of Science

Colorado State University

Fort Collins, Colorado

Summer 2015

Master's Committee:

Advisor: Karolin Luger

Susan Bailey
TingTing Yao

ABSTRACT

PARSING PARP: THE ENZYMATIC AND BIOPHYSICAL CHARACTERIZATION OF POLY (ADP-RIBOSE) POLYMERASES I and II

The ADP-ribosyl transferase (ART) family is a prominent group of at least seventeen enzymes comprised of mono (ADP-ribose) transferases (MARTs) and poly (ADP-ribose) polymerases (PARPs). Each family member contains a conserved PARP signature motif in the catalytic domain. Enzymatically active proteins, in the presence of co-factor NAD^+, catalyze individual or multiple ADP-ribose groups onto themselves or other proteins in automodification and heteromodification, respectively. The act of ADP-ribosylation implicates the ART family in a multitude of cellular processes including, but not limited to, transcription, apoptosis, DNA damage, metabolism, and inflammation.

The founding member of the ART family is PARP-1, a first responder to DNA damage and regulator of active gene expression. In its inactive state and as a chromatin architectural protein, PARP-1 tightly binds chromatin, thereby regulating cellular activities, signifying the importance of PARP-1 and chromatin interaction. Importantly, PARP-1 must be activated and automodified in order to bind histones and gain nucleosome assembly function. Structurally similar and in many ways thought to be functionally redundant, PARP-2 is also thought to primarily function in the DNA damage response. PARP-2 has a non-canonical DNA binding domain, and therefore it is able to recognize different types of DNA structures in comparison to PARP-1, which could suggest a unique role for PARP-2 in

repair. PARP-2 has not been extensively studied in a chromatin or gene regulation context due to this assumed redundancy.

Given the pronounced functional changes in PARP-1 upon automodification, it is important to better understand what exactly triggers its enzymatic activity. Similarly, due to the functional redundancy of PARP-2, insight into activators of its enzymatic activity could indicate specificity and selectivity for the protein. However, determining the details of nuclear components that activate PARP-1 and PARP-2 are limited by the availability of a reliable quantitative and kinetic assay, as well as by the availability of defined substrates. These limitations hinder the separation of potent, and thus biologically relevant, activators from weak or non-specific activators. Utilizing a fluorescence based enzyme assay adapted for this system, kinetic parameters of PARP-1 and PARP-2 allosteric activators are reported here. As proof of principle and to test the reliability of the enzymatic assay, PARP-1 and PARP-2 activity was first tested with nucleic acids and other previously reported activators, such as nucleosomes and histones. Next, potentially novel activators were tested.

Notably, PARP-1 is activated in the presence of its enzymatic product, PAR, indicating a mechanism by which PARP-1 could spread at sites of DNA damage and active gene expression. PARP-2 exhibits unique activation and specificity different from that of PARP-1 through its enzymatic preference for RNA. Further, PARP-1 remains the prominent chromatin related PARP due to the weak interaction, both activity and affinity, of chromatin with PARP-2. However, while PARP-1 and PARP-2 can act individually, affinity and activity studies demonstrate a PARP-1 and PARP-2 complex suggesting that these

proteins can act sequentially and simultaneously with one another during a PAR-mediated recruitment and signaling cascade. Overall, these data indicate novel functions and mechanisms for PARP-1 and PARP-2 within the nucleus as critical responders to DNA damage and gene regulation.

ACKNOWLEDGEMENTS

First and foremost, I would like to acknowledge and thank the Luger lab, most notably, Dr. Karolin Luger. Karolin took a risk by accepting an English major undergraduate into her lab, but helped to reignite the passion of science that I thought had been long extinguished. With that being said, my time in the Luger lab has been nothing short of a wonderful and exceptional, though at times very challenging, adventure. The 'PARP Team', Dr. Uma Muthurajan and Pam Dyer, deserve my extreme gratitude for their mentorship, support, and above all, friendship. Uma has been my mentor for the last four years and without her, I would not be the scientist nor the person I am today; my brief thank you cannot even begin to do her justice. For all the laughs, memories, and long days in the lab, I am forever grateful to all Luger lab members, past and present.

Next, I would like to thank my committee members, Dr. TingTing Yao and Dr. Susan Bailey for their helpful observations and perspectives throughout my Masters endeavor. Last, but definitely not least, I would like to acknowledge my family, my fiancé Andy, our cat Fitz, and our deaf dog Flurry. The struggle, and eventual triumph, through graduate school would not have been possible without them.

"I can no other answer make but thanks, and thanks, and ever thanks…"

- William Shakespeare, *Twelfth Night*

TABLE OF CONTENTS

LIST OF TABLES

LIST OF FIGURES

BIOLOGICAL RELEVANCE

The ADP-ribosyl transferases (ART) are a prominent nuclear family involved in a plethora of cellular processes ranging from DNA repair, gene expression, inflammation response, metabolism, and apoptosis. In humans, the ART family is composed of at least seventeen proteins with the ability to either mono (ADP-ribosyl)ate or poly (ADP-ribosyl)ate themselves or other diverse acceptor proteins in the presence of NAD^+. Notably, poly (ADP-ribose) polymerases I and II (PARP-1 and PARP-2) function within three main processes: transcription, DNA repair, and apoptosis.

Both PARP-1 and PARP-2 are modular proteins composed of a N-terminal DNA binding domain and a C-terminal catalytic domain. The primary difference in sequence and structure of PARP-1 and PARP-2 is in the N-terminal domain (N-PARP); PARP-1 has 3 zinc fingers, constituting a canonical DNA binding domain, while PARP-2 has a basic SAF-A/B, Acinus, and PIAS motif (SAP) domain, a non-canonical DNA binding domain. The catalytic domains (C-PARP) of PARP-1 and PARP-2 have a 69% sequence and structural homology. The NAD^+ binding site of PARP-2 has an additional three amino acid loop insertion, which lowers the specificity of PARP-2 for NAD^+. The difference of DNA binding domain and the NAD^+ docking site suggests that PARP-2 may have specific functions aside from PARP-1 redundancy.

Here I have developed a fluorescence-based enzymatic assay to quantify PARP-1/2 response to various allosteric activators. In addition, I have quantified the binding affinities

of PARP-1/2 to multiple nucleic acid and nucleosome constructs. These results herein indicate novel and specific functions of PARP-1 and PARP-2. Overall these data suggest enzymatically active PARP-1 interacts primarily with nucleosome constructs as a bona fide histone chaperone. PARP-2, on the other hand, has much weaker affinities for nucleic acids and chromatin than PARP-1. But PARP-2 is activated to a greater extent in the presence of single stranded RNA, as opposed to DNA, indicating a possible role of PARP-2 in transcription and RNA processing.

Lastly, while PARP-1 and PARP-2 function individually, they heterodimerize and elicit trans-activation. The preferred stimulation of activity by different activators (ss and dsRNA for PARP-2 and dsDNA for PARP-1) provides another layer of regulation to this interaction. The recruitment of PARP-2 and activity stimulation could provide a mechanism by which PARylation at sites of DNA damage or transcription remains more stable than the transient activation of PARP-1 alone. These data lead to better understanding of the specific and complex functions of PARP-1 and PARP-2 within the nucleus as first responders to DNA damage and gene expression.

Taken together, our results suggest a model wherein PARP-1 automodifies in response to cellular triggers and spreads across the site being activated by its own product and potentially recruits and/or activates PARP-2. PARP-2 in turn could subsequently be activated by RNA at sites of transcription.

BACKGROUND

I. ADP-Ribosyl Transferase Superfamily

Over 50 years ago, Chambon *et al.* identified a polyadenylic acid synthesizing enzyme activated in a DNA-dependent manner and in the presence of nicotinamide mononucleotide. This novel enzyme was originally found in calf thymus, pig liver, and rat liver but was missing in *E. coli (1),* although is now found in most cell types . The novel enzymatic product was later identified as poly (ADP-ribose) (PAR) and sparked the field of research on poly (ADP-ribosyl)ation (Figure 1A).

PAR is composed of long branched chains of ADP-ribose monomers that are joined by glycosidic linkages and these chains can be as long as 200 monomeric units in the cells; proteins that catalyze PARylation were aptly named poly (ADP-ribose) polymerases or PARPs (Figure 1A). PARPs, in the presence of co-factor and substrate NAD^+, catalyze long chains of PAR onto themselves or other acceptor proteins during auto- and heteromodification, respectively. PAR most commonly covalently links onto glutamic acid residues but lysines and aspartic acids are also known to accept ADP-ribose groups; however, there is no recognition sequence, a requirement for histone acetyl transferases, for example. Initially, proteins accept a single mono (ADP-ribose) group and this group can then be elongated and branch into chains of poly (ADP-ribose) (2).

From the original discovery of PAR and PARPs, the prominent nuclear PARP superfamily was formed. This family consists of seventeen PARP homologues; however, because not

A.

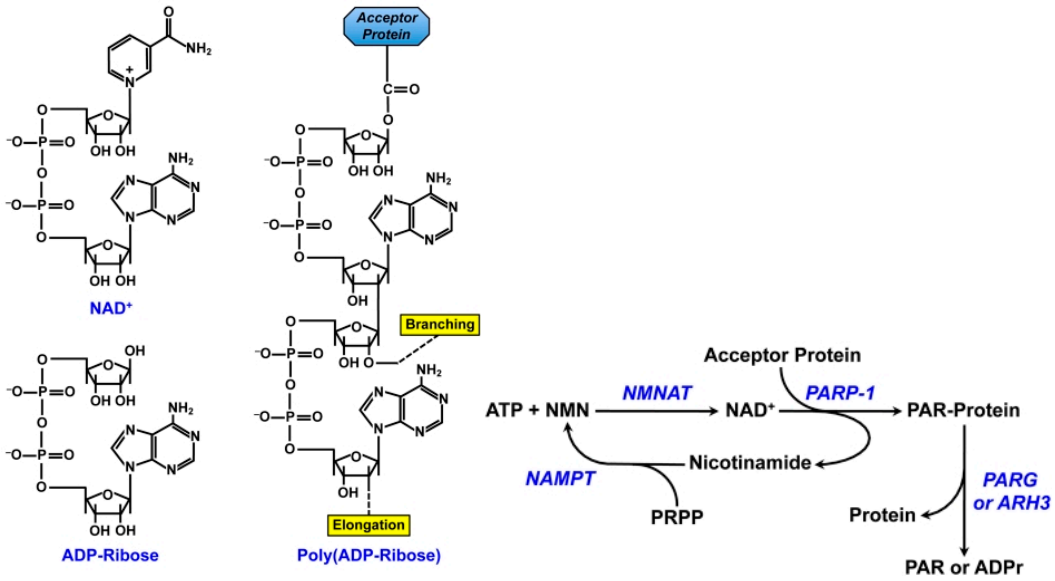

B.

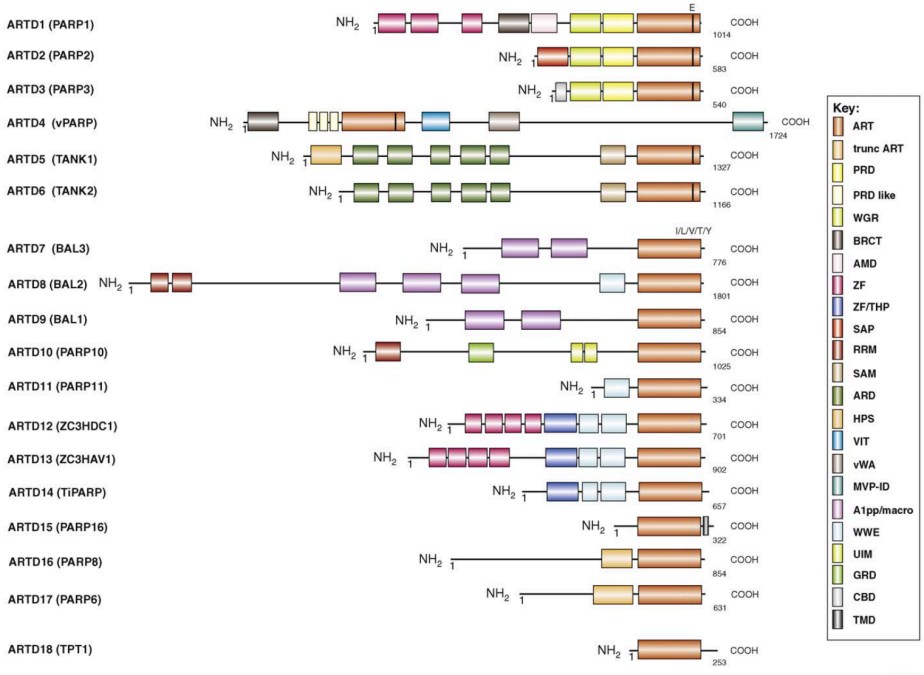

Figure 1: The ART family catalyzes ADP-ribosylation reactions in the presence of NAD⁺.

- **A.** The structure and mechanism of poly (ADP-ribosyl)ation by PARPs; PAR is hydrolyzed by poly (ADP-ribose) glycohydrolase (PARG). Adapted from (3).
- B. Schematic of the domain architectures of the ART family members. Common motifs are as follows. ART: ADP-ribosyl transferase; ZF: zinc fingers; PRD: PARP regulatory domain; ARD: ankyrin repeat domain; WWE: three conserved residues (W-W-E). Adapted from (4).

every protein within the family has poly (ADP-ribosyl)ation activity, the family nomenclature has been modified to properly reflect all the homologues and is now named the ADP-ribosyl transferase (ART) family (4). Naming of each family member was changed from PARP to ADP-ribose transferase diphtheria toxin-like (ARTD) followed by each respective number. However, since this study only focuses on poly (ADP-ribose) polymerases, the old nomenclature of 'PARP' will be employed.

This family is composed of four sub-families: DNA-dependent PARPs (PARP-1, PARP-2, and PARP-3); tankyrases (PARP5a, tankyrase-1 and PARP-5b, tankyrase-2); RNA binding PARPs (PARP-7, PARP-12, PARP13.1, PARP-3.2); macroPARPs (PARP-9, PARP-14, PARP-15) (Figure 1B) (5). Formation of PAR is involved in protein-protein interactions, mitochondrial functions and a variety of stress responses, thus indicating the importance of the ART family in a majority of critical cellular processes.

II. Poly (ADP-Ribose) Polymerase I & II

The founding, and therefore most extensively studied, member of the ART family is ADP-ribosyl transferase diphtheria toxin-like 1, herein referred to as poly (ADP-ribose) polymerase I (PARP-1). This abundant nuclear enzyme is the second most prominent protein in the nucleus, second only to histones. On average, cells contain $1x10^6$ PARP-1 molecules; this concentration corresponds to about 1 PARP-1 molecule to every 20 nucleosomes. PARP-1 is also ubiquitously expressed in most organisms from plants and *C. elegans* to higher order organisms, frogs and humans, but is notably missing in yeast (6). Due to the expansive research on PARP-1 structure and function, the structure for PARP-1

subdomains, with and without enzymatic inhibitors, are now well characterized with a variety of NMR solution state and x-ray crystallography structures. Structurally, PARP-1 is a multi-domain protein with 6 modular domains: the N-terminus DNA binding region composed of 3 zinc fingers and an automodification domain containing BRCA C-terminus fold; the catalytic C-terminus composed of a WGR domain, and the catalytic domain, consisting of a helical subdomain and an ADP-ribosylation (ART) subdomain (Figure 2A) (7, 8).

In general, PARP-1 enzymatic activation and ADP-ribosylation accounts for the majority of PARylation and NAD^+ usage within the cell (9). The accumulation of PAR is embryonically lethal and serves as a signal for programmed cell death, which is discussed in more detail later in this chapter. Furthermore, PAR formation eventually serves as a negative feedback inhibitor of PARP-1 due to its highly branched polymer chain and accumulation of negative charge, PARP inhibition helps slow consumption of cellular NAD^+ stocks (10).

Over 90% of the ADP-ribosylation *in vivo* is covalently linked to PARP-1 through automodification making PARP-1 an atypical enzyme (11, 12). Automodification of PARP-1 and the resulting long PAR chains act as a signal for transcription factors and DNA repair factors – a similar mechanism as would be seen with a scaffolding protein, for example. Once DNA repair and transcription factors are recruited, PARP-1 assists in the assembly of transcription or repair complexes.

A.

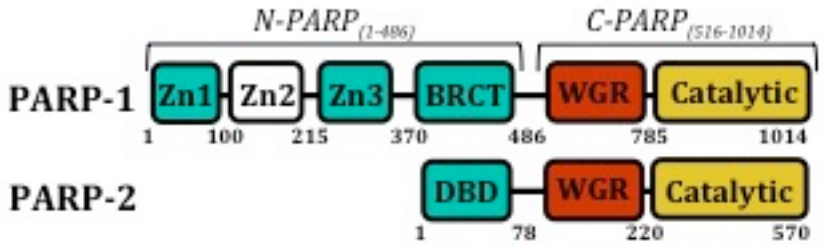

B.

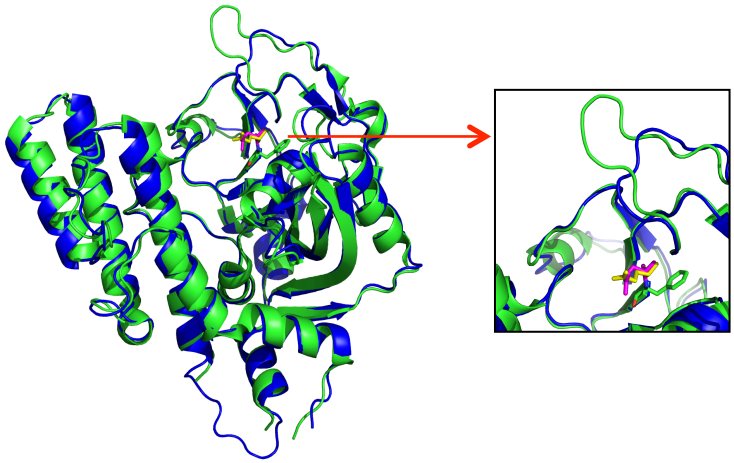

Figure 2: Modular domain structure of PARP-1 and PARP-2.

- **A.** PARP-1 and PARP-2 are multi-domain proteins composed of a DNA binding N-terminus and a catalytic C-terminal domain (C-PARP). The N terminal domain (N-PARP) of PARP-1 contains 3 DNA binding zinc fingers and BRCA C-terminus fold and C-PARP-1 is composed of a WGR domain and a catalytic domain with a helical domain and an ADP-ribosylation transferase domain. The N-PARP-2 has a SAP DNA binding domain and C-PARP-2 also has a WGR and a catalytic domain. Adapted from (13).
- **B.** The crystal structure of PARP-1 (blue, PDB: 1A26) and PARP-2 (green, PDB: 1GS0) catalytic domain; the catalytic domains have a 70% sequence similarity. The active site is enhanced in the box on the right with the PARP motif highlighted in yellow (PARP-1 E988) and magenta (PARP-2 E534). Adapted from (12, 14)

Primarily studied through the lens of DNA damage repair, the best understood activator of PARP-1 enzymatic activation is DNA with available base pair ends. Further, the crystal structure of PARP-1 in complex with double stranded DNA has been solved (8). Zinc finger 1 (Zn1) and zinc finger 2 (Zn2) are required for the DNA binding activity of PARP-1, while zinc finger 3 (Zn3) is required for DNA-dependent catalytic activity (15, 16). In complex with DNA, the WGR domain interacts with Zn1, Zn3, and the CAT domain as the signaling bridge between the N-terminal domain and C-terminal domain of PARP-1. Specifically, the helical domain (HD) transmits the signal from the WGR into the ART portion of the catalytic domain. Upon DNA binding, PARP-1 collapses on itself forming a compact structure in which the automodification domain is in close proximity to the ART domain consistent with the preference of PARP-1 to automodify rather than heteromodify.

For many years, PARP-1 was considered the only cellular protein capable of ADP-ribosylation. In 1998, Shieh *et al.* discovered the presence of DNA-dependent PAR activity in PARP-1 null ($PARP^{-/-}$) mouse embryonic fibroblasts (17). This discovery suggested additional PARP proteins other than the canonical PARP-1. Specifically the knockout mice showed normal fetal development but were highly sensitive to DNA damage and genomic instability, an expected defect due to the known role of PARP-1 in DNA damage. What was unexpected, however, is the mice were viable and had regular growth, in addition to PAR activity.

One year later, Amé *et al.* named the newly discovered PARP protein, ADP-ribosyl transferase diphtheria toxin-like 2, herein referred to as PARP-2 (18). In this early

structural study, Amé *et al.* assigned the PARP-2 gene to chromosome 14, which differs from PARP-1 found on chromosome 1. Interestingly in humans and a few species of monkeys, the PARP-2 gene is alternatively spliced to form a shorter and longer isoform (19). The differing isoforms are not present in other organisms containing PARP-2 and moreover, PARP-2 is altogether absent in avian species.

PARP-2 is much shorter than PARP-1 (535 amino acids and 1014 amino acids, respectively), but as with PARP-1, can also be divided into two domains, a DNA-binding N-terminal domain and a catalytic C-terminal domain (Figure 2A). Overall, PARP-1 and PARP-2 share a 40% sequence homology and 70% similarity (Supplementary Figure 14). The differences between the two proteins are located mostly to the N-terminal domain, the DNA binding region. Unlike PARP-1 with 3 DNA binding zinc fingers, PARP-2 has a SAP domain, a non-canonical DNA binding domain. The SAP domain is named for the SAF-A/B, Acinus, and PIAS motifs; the SAF-A/B motif arises from scaffold attachment factors, Acinus is a chromatin associated protein, and PIAS is an example of STAT inhibitors involved with DNA repair (20). Sequence specific, SAP motifs are groups of conserved hydrophobic, polar, and bulky amino acids and are predicted to be alpha helical. Notably, the SAP domain is also found in PARP-1 and PARP-2 plant orthologs (20). In addition to the SAP domain, the N-terminus of PARP-2 is rich in basic amino acids, 27% lysine or arginine (21).

PARP-2 has a WGR domain, similar to PARP-1, but is missing an automodification BRCT domain; nonetheless, PARP-2 has the capability of auto- and heteromodification. The amino acid sequence and structure of the catalytic domain of PARP-2 is very similar to that of

PARP-1. PARP-1 and PARP-2 have a 69% sequence (Supplementary Figure 14) and structural similarity (RMSD: 0.834) in terms of the catalytic domain (human PARP-1: 518-1014; mouse PARP-2: 209-557) (22). The primary differences in the catalytic domains are the narrower catalytic cleft and the insertion of a three amino acid loop within the active site of PARP-2 (Figure 2B). Additionally, in this insertion, PARP-2 contains Y528, which has no corresponding residue in PARP-1, and lies within the PAR elongation region, an active site separate from PAR initiation. (14, 22). This insertion lowers the affinity of PARP-2 for NAD^+, thereby making PARP-2 a less efficient enzyme when compared to PARP-1 (14). However, independent functions of PARP-2 and any PARP-1 dependent functions of PARP-2 are not well characterized; what is known and reported in literature so far is summarized below.

The diversity of PARP-1 and PARP-2 as nuclear enzymes is reinforced in their functions within the cell. Specifically, both proteins are known to function in the nucleus in, primarily, four distinct ways and each of these are discussed below:

1. Chromatin Dynamics
2. Transcription
3. DNA Repair
4. Apoptosis

i. Chromatin Dynamics

In eukaryotic cells, each cellular nucleus has to accommodate over two meters of DNA. The most basic unit of DNA packaging is the mononucleosome; the nucleosome coordinates 146

base pairs of left handed supercoiled DNA by wrapping it 1.65 times around a core histone octamer (23). Specifically, the octamer is composed of two (H2A-H2B) dimers and one $(H3\text{-}H4)_2$ tetramer; each histone has an ordered alpha helical core involved in DNA binding while disordered N-terminal tails interact with other nucleosomes and nuclear proteins. Once assembled, mononucleosomes are arranged in array of nucleosomes similar to beads on a string and from each string, higher order chromatin structures are condensed into the chromosome. The process of DNA packaging is facilitated by a multitude of proteins including linker histones and architectural proteins (Figure 3A).

At the very basic level, chromatin dynamics control a variety of processes from gene expression and DNA replication to DNA damage repair and recombination. During these processes, the DNA must be unwrapped in order to be available for interaction with other nuclear protein complexes (24). To accomplish this, nucleosomes need to be disassembled, partially or completely, and then reassembled once the repair or transcription process is complete. Nucleosome assembly and disassembly is facilitated by histone chaperones, a class of proteins that have a high affinity for histones and regulate nucleosome assembly (e.g. Nuclear Assembly Protein, Nap1). Histone chaperone function is dependent upon histone post-translational modifications, nucleosome structure, and other nuclear machinery, such as polymerases (25-27).

Nucleosome disassembly is necessary for transcription initiation and elongation. While eukaryotic cells have predominately evolved to have transcription start sites in

A.

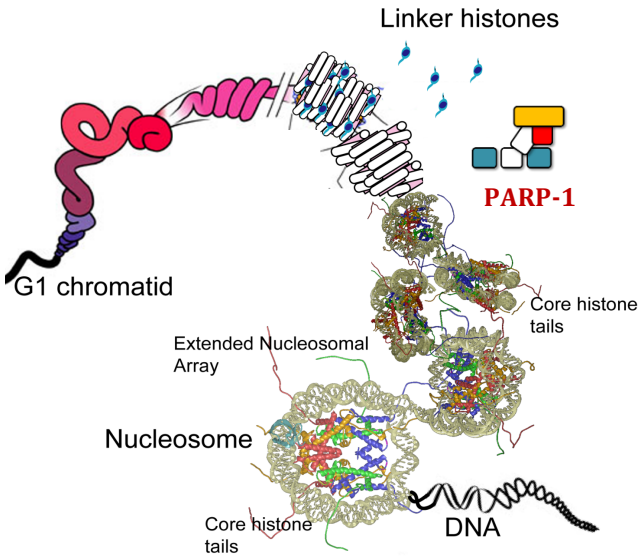

B.

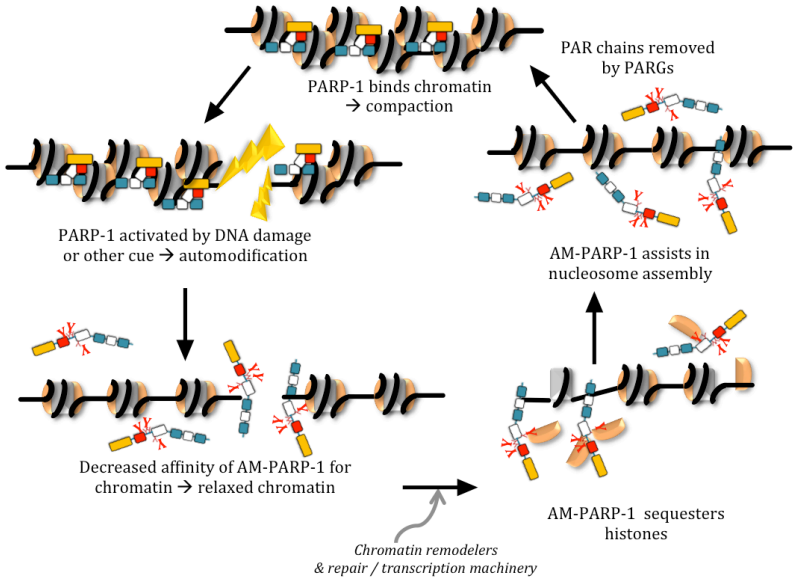

Figure 3: The two functional modes of PARP-1 as a chromatin architectural protein and a histone chaperone.

- **A.** As a chromatin architectural protein, PARP-1 condenses nucleosomes to help package DNA into chromosomes. Adapted from (28).
- **B.** PARP-1 switches from architectural protein to a histone chaperone by losing affinity for chromatin and gaining affinity for histones as well as nucleosome assembly function. Adapted from (29).

nucleosome free regions (NFR), the nucleosome barrier becomes apparent during elongation (30, 31). Teves *et al.* describe two major ways cells overcome the nucleosome barrier: chromatin modifiers and chromatin remodelers (31). First, chromatin modifiers are histone modifications, such as PARylation, and specific histone variants, such as H3.3. Modifications and variants yield a more open nucleosome thus breaking histone-DNA contacts allowing a nucleosome to be more easily disassembled. Second, chromatin remodelers are ATP-driven nuclear proteins that slide nucleosome along the DNA, evict histones, exchange canonical histones for histone variants, or evict the entire octamer (30). In addition to chromatin remodelers, this last category would encompass the class of histone chaperones previously described.

On the other end of the spectra, negating the chromatin dynamics induced by the remodelers and chaperones are the chromatin architectural proteins, like PARP-1, that compact chromatin and thereby contribute to transcription regulation (32, 33). In its inactive form, PARP-1 serves as a chromatin architectural protein that is able to bind a variety of nucleosomes with tight nanomolar affinities (7) (Figure 3A). PARP-1 condenses chromatin in a similar manner to linker histone H1 (34). Specifically, during MNase protection assays, PARP-1 was shown to bind nucleosomes at the dyad exit and entry region next to the linker DNA (35). Moreover, PARP-1 is enriched at transcription start sites (36). Wacker *et al* reinforce the role of PARP-1 as a chromatin architectural protein since PARP-1 is necessary for nucleosome binding, compaction, and thus, transcription repression (32).

PARP-1 embodies two distinct modes of interaction depending on its binding partner, chromatin or DNA. While the first and third zinc fingers have been implicated in DNA binding (7, 8), the second zinc finger and the WGR-CAT domains may be required for PARP-1 interaction with chromatin (7). Recently, Muthurajan *et al.* quantified a second binding mode of PARP-1 to nucleosomes (29). In the presence of higher order chromatin, trinucleosomes, PARP-1 exhibits a low nanomolar affinity to trinucleosomes without exposed DNA linker ends; atomic force microscopy images show PARP-1 compacting trinucleosomes by redirecting linker DNA between the nucleosomes. Additionally, qualitative studies (e.g. electrophoretic mobility shift assays) show PARP-1 binding to a circular chromatin template (35). Thus, in addition to interacting with damaged chromatin, PARP-1 interacts with non-damaged chromatin to promote genome wide PARP-1 binding as well as chromatin condensation.

In addition, Muthurajan *et al.* characterized a switch in PARP-1 function upon enzymatic activation and subsequent automodification. Upon PARP-1 activation, PARP-1 loses affinity for chromatin, but not for free DNA, while simultaneously gaining affinity for histones and acquiring nucleosome assembly function. The high affinity for histones and nucleosome assembly function fits the definition for a bona fide histone chaperone. Thus, PARP-1 is the first histone chaperone that gains this function due to an enzymatic switch (Figure 3B). The enzymatic switch of PARP-1 between chromatin architectural protein and histone chaperone further elucidates the critical role of PARP-1 in DNA damage repair and gene expression. However, the exact details of which nuclear components cause this switch are not well understood.

Unlike the extensive studies of the role of PARP-1 in chromatin dynamics, PARP-2 function is unexplored and not well characterized. This is primarily due to PARP-2 only accounting for 5-10% of the PARP activity in the cell so it has therefore been assumed to be, in many ways, functionally redundant to PARP-1 (18). The number of published studies of PARP-2 in specific context with chromatin are extremely limited – and these primarily report PARP-2 and chromatin in the context of centromeres, telomeres, and during spermatogenesis.

Firstly, during mitotic division, both PARP-1 and PARP-2 accumulate at the centrosome in a cell cycle dependent manner (19). Here, unlike PARP-1 with a broad and general chromatin interaction, PARP-2 specifically interacts with kinetochore proteins A and B as well as with the mitotic spindle checkpoint protein, BUB3 (37-39). Overall, it is suggested that PARP-2 has a role in chromosome segregation due to the increased accumulation of PARP-2 at the centromere when microtubule dynamics are faulty – Yelamos *et al*. equate this PARP-2 behavior to be characteristic of a spindle checkpoint protein (37, 38). Additionally, in PARP-2$^{-/-}$ cells, the kinetochore is defective in response to DNA damage causing mis-segregation of the chromosome, reinforcing the role of PARP-2 in maintaining centromeric chromatin (37, 38).

Secondly, PARP-2 is implicated in the maintenance of telomeric heterochromatin. PARP-2 interacts with telomere repeat binding factor 2 (TRF2) in both a functional and specific manner (37, 40). TRF2 is similar to PARPs in that it has a crucial role in telomeric DNA repair and recruitment of repair proteins. PARP-2 then regulates the DNA binding activity

of TRF-2 through PARylation of this telomeric protein. It was later published that PARP-1 may also play a role in this interaction, although it is unclear whether PARP-1 and PARP-2 function individually or synergistically in telomeric maintenance (41).

Thirdly, PARP-1 and PARP-2 are known to function in chromatin remodeling during mouse spermatogenesis mediated by the interaction with topoisomerase IIβ (42, 43). PARP-1 and PARP-2 inhibit the topoisomerase activity by discouraging DNA break formation during sperm development. Both PARP-1 and PARP-2 may be active during spermatogenesis facilitating H1 removal and chromatin relaxation, thus allowing for remodeling to occur. However, the specific functions of PARP-1 and PARP-2 during this process are not understood.

In terms of modulating chromatin and its dynamics, PARP-1 is the prominent PARP involved in chromatin condensation and ADP-ribosylation in the nucleus. Serving two distinct functions, depending on an enzymatic switch, PARP-1 functions as a chromatin architectural protein and a histone chaperone able to assemble nucleosomes. PARP-2 may serve a more important and necessary role here, but this is unknown currently.

ii. Gene Expression & Transcription

The idea that PARP-1 plays key roles in transcription regulation and gene expression has gained momentum in the last decade. It is proposed that PARP-1 regulates transcription in two distinct modes: independent of its enzymatic activity and PAR dependent. The enzymatically independent role of PARP-1 was described in the previous section on

chromatin dynamics. Here, the function of the PAR modification itself in transcription will be reviewed.

In addition to its role as a chromatin architecture protein, PARP-1 also plays a role in chromatin relaxation (44). When PARP-1 becomes automodified, it loses affinity for non-damaged nucleosomes causing PARP-1 to release chromatin – this release would thereby yield chromatin relaxation. Tulin *et al.* further describe PARP-1 activation leading to decondensation of chromatin at PARP-1 regulated genes. At a heat shock responsive *Drosophila* gene, puffing of loci was recorded upon PARP-1 activation and subsequent PAR accumulation (45). Importantly, a PARP-1 catalytically inactive mutant was not able to recapitulate the puffs – PARP-1 activity is therefore critical for chromatin decondensation.

Importantly, the loosening of chromatin and nucleosome disassembly will allow access of the transcription machinery and thus, allow the elongation process to proceed. Petesch and Lis, also studying *Drosophila* heat shock genes, published a study in which the spread of PARP-1 and PAR at activated heat shock genes simultaneously caused nucleosome loss over the gene (46). Likewise, the rate at which nucleosomes were lost over the gene corresponded with the rate of PARP-1 spreading (30, 46, 47). Specifically, nucleosome loss that occurs two or more minutes after the initial heat shock is directly related to transcription; therefore, both the transcription independent and dependent loss of nucleosomes is correlated with PARP-1 spreading and its catalytic activity. However, the mechanism of this PARP spreading is not known.

Although 90% of PAR found *in vivo* is covalently linked to automodified PARP-1 (48), PARP-1 is also known to heteromodify histones, particularly histone H1 and H2B (35, 49, 50). The PARylation of histones furthers chromatin relaxation due to the electrostatic repulsion of PAR and DNA, both negatively charged. Further, PARylated histones repel other transcription or nuclear factors from interacting with histones; for example, PARP-1 may inhibit demethylation of histone H3K4 trimethylation by preventing KDM5B histone demethylase from binding its substrate (51).

Similarly, PARP-1 directly modifies transcription factors influencing both their activity and cellular location. Specifically, PARP-1 has been studied for its interaction with nuclear factor, NF-κB. The PARP-1 and NF-κB interaction is an example of enzymatic independent PARP-1 transcription; however, in addition, NF-κB drives PARP-1 enzymatic activity (52).

During RNA synthesis, the function of PARP-1 in RNA regulation and processing is a new and exciting field of PARP research. Studies suggest PARP-1 is involved in the synthesis of non-coding RNAs, ribosomal biogenesis in the nucleolus, and mRNA processing. PARP-1 has been shown to interact with the nucleolar remodeling complex, NoRC which functions in rRNA gene transcription and yields transcriptional silencing (5). More specifically, PARP-1 PARylates TIP5, a subunit of NoRC, suggesting that PARylation plays a role in silencing ribosomal chromatin. Likewise, PARP-1 is implicated in RNA processing as a regulator of alternative splicing and has been shown to interact with a variety of splicing factors (53). Apart from interaction of PARP-1 with splicing factors, a number of studies have described additional functions of PARP-1 in RNA splicing. For example, Ji and Tulin

show the PARylation of *Drosophila* hnRNPs regulates splicing by shifting its specificity of RNA binding (54).

Similar in many ways to PARP-1, the function of PARP-2 in transcription is slightly more understood. Enzymatically active PARP-2 modifies the activity of transcription factors such as SIRT1 and TTF-1 (55). In its interaction with SIRT1, PARP-2 directly regulates SIRT1 by binding the SIRT1 promoter and repressing transcription. Nevertheless, unlike PARP-1, which controls transcription in an ADP-ribosylation dependent manner, PARP-2 also regulates transcription through histone deacetylation and methylation (56). Importantly, PARP-2 controls transcription repression by recruiting histone deacetylases (HDAC5 and HDAC7) as well the G9a, a histone methyltransferase. These proteins are specifically recruited to cell cycle related genes yielding heterochromatin and transcription repression.

Recently, Léger *et al.* reported that PARP-2 enzymatic activity is greatly stimulated by RNA, to an even greater extent than was reported for PARP-1 (57). Utilizing mouse ribosomal RNA, Léger and colleagues show two important findings. First, as studied using radioactive NAD^+, PARP-2 is enzymatically stimulated 3-fold stronger than was visualized with double stranded DNA while PARP-1 exhibited a 0.7-fold decrease. Second, this interaction occurs through the SAP domain of PARP-2. This study provided the first glimpse into the role of PARP-2 enzymatic activity in RNA processing.

Similar to chromatin dynamics, PARP-1, again, serves as the prominent PARP protein during transcription activation and repression. Both PARP-1 and PARP-2 ADP-ribosylation

is implicated in regulation and modification of various transcription factor activity and plays a role in RNA processing. However, specific functions of PARP-2 in transcription need to be further explored.

iii. DNA Damage Repair & Signaling

Structural basis for DNA binding by PARP-1 and PARP-2

In 2012, Langelier *et al*. published the groundbreaking structure of PARP-1 (Zn1, Zn3, and WGR-CAT domains) in complex with double stranded DNA (Figure 4A). Specifically, Zn1, Zn3, and the WGR domains collapse and bind to double stranded DNA breaks (Figure 4A, boxed inset). Zn1 and WGR are predominately involved with binding while Zn3 is crucial for DNA-dependent activation of PARP-1 (Figure 4B). Serving as the regulatory domain, the WGR domain transmits the binding signal through the helical subdomain (HD) to the ADP-ribosyl transferase (ART) subdomain. This signal serves as the activation signal connecting the DNA binding N-terminal domain and catalytic C-terminal domain of PARP-1. The collapse of PARP-1 onto a DNA end allows for the catalytic domain to change conformation and become active, accepting NAD^+ into the active site for PARylation reactions.

Upon closer examination of the crystal structure, it is apparent that the PARP-1 and DNA interaction is dependent upon a double stranded helix. Removing a single strand of DNA from the crystal structure shows two possible scenarios (yellow or orange strands, Figure 4A and 4B). A single stranded DNA will interact with either Zn1 (orange strand) or WGR (yellow strand) and in b1oth scenarios, single strands will only partially interact with Zn3.

A. **B.**

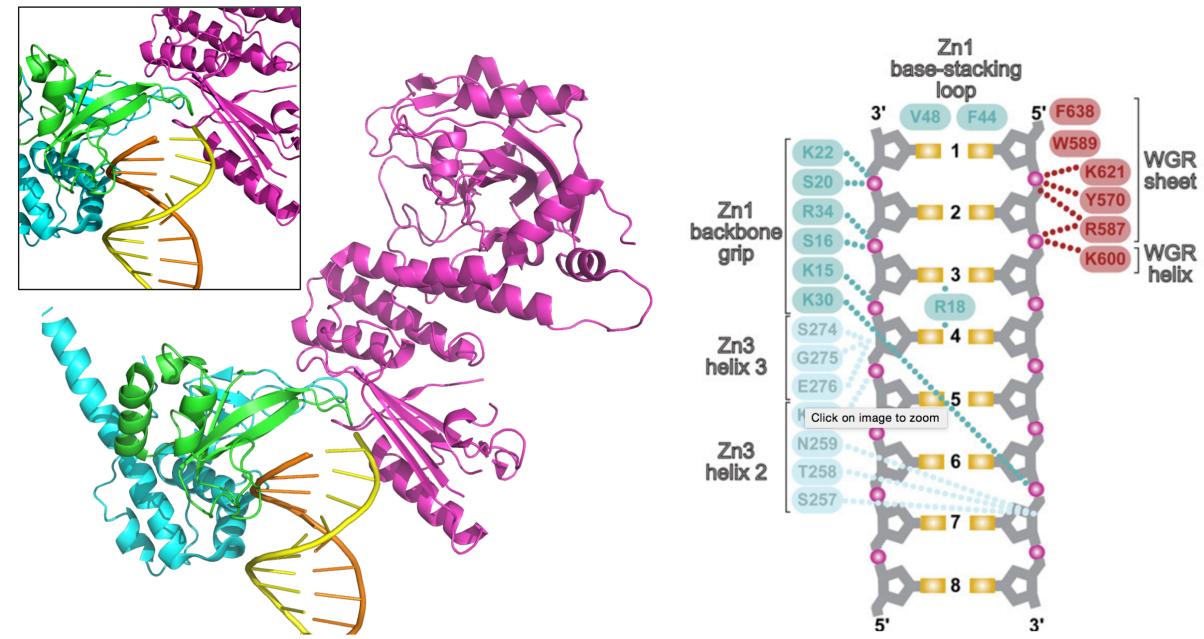

C.

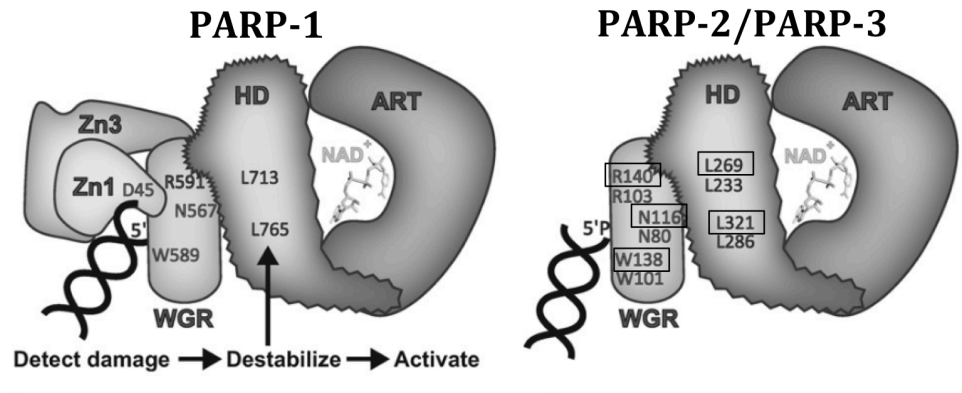

Figure 4: Structural basis of PARP-1 and PARP-2 binding DNA
A. Crystal structure of PARP-1 binding DNA (PDB: 4DQY). Zinc finger 1 (green) and the WGR (magenta) domains are involved with DNA binding while zinc finger 3(cyan) is involved with DNA-dependent activation. Adapted from (8).
B. Specific residue interactions of PARP-1 and DNA from 4A.
C. Model of PARP-1 (left) and PARP-2 (right, boxed residues) DNA-dependent binding and activation. PARP-1 zinc fingers (Zn) and WGR collapse onto DNA upon binding. The binding signal is transmitted from the WGR to the ADP-ribosyl transferase (ART) through the helical domain (HD). PARP-2, on the other hand, binds DNA through its WGR domain, which then transmits the signal through the HD domain to the catalytic ART subdomain. Residues that are involved in critical interactions (either protein-protein or protein-DNA) are indicated. Adapted from (13).

The decrease in interactions for single stranded DNA could shift both the activity and specificity for single stranded nuclei acids, including RNA.

Two years later and with no solved crystal structure of PARP-2 in complex with DNA, Langelier *et al.* published a study exploring the DNA-dependent enzymatic activation of PARP-2 as well the structural basis for this interaction. Unlike PARP-1, which requires a full base pair in order to be activated by DNA (8), PARP-2 only requires a 5' phosphate (13). Moreover, while PARP-1 requires the N-terminal domain for DNA-dependent activation (specifically Zn3), the enzymatic region of PARP-2 is the WGR domain (Figure 4C). When tyrosine 188 (polar) in the PARP-2 WGR was mutated to a phenylalanine (non-polar), DNA-dependent activity was lost and a significant reduction in DNA binding affinity was reported (7% of the wild type). This data suggests that the non-canonical DNA binding domain of PARP-2, together with the lack of zinc fingers, shift the DNA binding interface from the N-terminus to the WGR domain. In short, the WGR domain of PARP-2 replaces zinc finger 3 domain of PARP-1 for the regulation of DNA binding. Further when asparagine 116 (polar), a residue at the interface between WGR and the HD domain, was mutated to an alanine (non-polar), DNA-dependent activity was also diminished. However, this mutation (N116A) yielded only a slight deficiency in affinity (45% of the wild type). This data suggests that similar to PARP-1, the communication bridge between the WGR domain and the HD subdomain is required in PARP-2 DNA-dependent activation but DNA binding.

Overall, the initial binding of DNA to PARP-1 and PARP-2 is drastically different. While PARP-1 relies on zinc finger and WGR interaction, PARP-2 binding is mediated solely by the

WGR, not the N-terminal domain. Similarly, though, both proteins rely on the collapse of structure and signaling bridge from the WGR to the catalytic domain via the HD subdomain. The different in domains involved with DNA binding could suggest differences in activation and affinity for PARP-1 and PARP-2 in the presence of various nucleic acid substrates.

PARP-1 and PARP-2 function in single stranded break repair

While PARP-1 was primarily studied for its role in DNA damage repair and signaling due to its ability to bind damaged DNA (single and double strand breaks), supercoils and cruciform DNA (7, 13, 58), PARP-1 does not have a direct function within DNA repair but serves as a coordinating and signaling factor. Thus, overall PARP-1 is a critical component in genomic integrity; for example, in mouse PARP-1 knockouts, future generations exhibit hypersensitivity to UV and ionizing radiation all leading toward rapid and uncontrolled DNA damage (59). PARP-1 functions in base excision (BER), nucleotide excision (NER), mismatch (MMR), single-strand break repair (SSBR), and also in non-homologous end joining (NHEJ), and homologous recombination (HR).

In BER, PARP-1 is known to interact with apurinic and apyrimidinc (AP) sites to mark nicked DNA locations, which in turn enhance PARP-1 automodification and allow a DNA repair signaling to be propagated (60). PAR recruits repair factors ranging from XRCC1, PNK, and DNA polymerases. PARP-1 involvement in NER and MMR is not as well characterized. It is speculated that PAR is able to interact with a variety of proteins implicated in these processes; nevertheless, it is not known whether this is through PAR attached to PARP-1 or to another acceptor protein (61).

As the other main PARP involved in DNA damage, PARP-2 has also been extensively studied for its role in DNA damage repair and here, distinctive features are apparent. In single strand break repair, PARP-2 favors binding to gaps and flaps in the DNA structure suggesting it may have a role in the later steps of repair, such as DNA ligation (22). In BER repair, PARP-2 interacts with XRCC1, DNA Polymerase β, and DNA ligase III – all known binding partners of PARP-1. Although the binding partners are similar between PARP-1 and PARP-2, mouse embryonic cells with a PARP-2 knockout have defective BER pathways; therefore, PARP-2 is required in this pathway (62). More recently, Kutuzov *et al.* quantified the affinities of PARP-2 to BER DNA intermediates; PARP-2 exhibited the highest affinity for flap containing DNA structures (63). Interestingly, while PARP-2 binds the tightest to DNA with flaps, it is most efficiently activated by a 5' overhang structure reinforcing that like in the case of PARP-1, enzymatic activity and binding affinities are not always correlated (13). In addition, PARP-2 enzymatic activity is not necessary for DNA synthesis and repair.

PARP-1 and PARP-2 function in double strand break repair

More recently, the role of PARP-1 in double strand break (DSB) repair, both NHEJ and HR, has been explored. During canonical NHEJ, Ku and DNA-PKcs control repair of the DSBs. While PARP-1 has been shown to interact with Ku and DNA-PKcs, PARP-1 is not implicated in the classical NHEJ repair pathway. Instead, it is proposed that PARP-1 participates in an alternative NHEJ pathway (64). Here, ADP-ribosylation of repair factors is crucial for repair success. This alternative pathway occurs independently of both Ku and DNA-PKcs; furthermore, it is thought that this pathway may breakdown to several other sub-pathways.

In NHEJ, PARP-1 serves as a scaffold to recruit and assemble large DNA repair complexes, as previously stated (65, 66).

The role of PARP-1 in homologous recombination (HR) is slightly more understood. Specifically, PARP-1 PARylation recruits Ataxia Telangiectasia Mutated (ATM), a prominent player in DSB repair known to phosphorylate the histone variant, H2AX. ATM and phosphorylated H2AX (γH2AX) serve as signals of DNA damage and cell cycle arrest. Interestingly, a double knockout of PARP-1 and ATM, or PARP-1 enzymatic inhibition, causes embryonic lethality in mice suggesting a necessary interaction between the two proteins (37, 61). Schultz *et al. s*how PARP-1 inhibition does not interfere with HR repair but loss of PARP-1 induces hyper recombination. Thus, PARP-1 orchestrates and coordinates repair without having a critical role within the pathway (67).

Disrupting the functional interaction of PARP-1 with ATM causes further delayed downstream effects, most notably with the tumor suppressor protein, p53. Like ATM, PARP-1 interaction with p53 is mediated by PAR and hence its enzymatic activity. Nguyen *et al.* found that disruption of PARP-1 enzymatic activity further affects p53 function by interfering with p53 signaling pathways (68). In addition, ARF, another tumor suppressor gene, is also influenced by PARylation, PAR chains initialize transcription of the gene. (69).

In conjunction with PARP-1, PARP-2 is implicated primarily in single stranded break (SSB) repair but some important associations have been made for its connection to DSB repair. Similar to PARP-$1^{-/-}$ and $ATM^{-/-}$ knockouts being embryonically lethal, a PARP-$2^{-/-}$ and ATM-

/- double knockout is also lethal (70). Here PARP-1 and PARP-2 cannot compensate for the loss of the other since both double knockouts (PARP-1 and ATM; PARP-2 and ATM) are lethal, likely due to the inefficient SSBR/BER pathways. This phenomenon highlights the DNA repair specificity of PARP-1 and PARP-2.

Overall, within the realm of DNA damage repair, PARP-1 and PARP-2 take on unique roles to increase genomic stability and DNA repair. PARP-1 serves as a coordinating and signaling protein during initial recognition of a break, while PARP-2 seems to primarily function during later steps of repair, such as ligation. Importantly, both proteins are crucial for DNA damage repair in cell, rather than exhibiting functional redundancy.

iv. Apoptosis & Cell Death

Apoptosis is the process of programmed cell death that is required for survival of multi-cellular organisms. This process is stimulated by a proteolytic cascade, which allows the cell to die without harming surroundings cells, as opposed to necrosis. Caspases (cysteine-aspartate directed proteases) are initially inactive before being cleaved into their active form as procaspases. Activated caspases then cleave and activate other effector caspases. Once activated, effector caspases are able to cleave their catalytic targets.

During the beginning of apoptosis as part of the "PARP suicide hypothesis", *in vivo* PARP-1 is quickly cleaved by caspase 3 and 7 but *in vitro*, PARP-1 is cleaved by any caspase. The caspase-3 cleavage sites in human PARP-1 are as follows: DEVD (210-213), DGVC (213-216), DPID (787-790), and DGVD (964-967); however, the Asp-x-x-Asp motif of DEVD is

most commonly cleaved (71). While caspase 3 cleaves PARP-1 regardless of automodification activity (72), PARP-1 is most often cleaved due to high levels of PARP-1 automodification. The over-activity of PARP-1 leads to NAD^+ depletion and eventual necrosis of the cell. The proteolysis of PARP-1 by caspase 3 and 7 cleaves the protein into the N-terminal and C-terminal domain halves thereby diminishing DNA-dependent catalytic activity; the catalytic domain of PARP-1 is not constitutively active and only exhibits basal activity when cleaved (48). The N-terminal domain retains DNA-binding without catalytic activity therefore locking PARP-1 onto damaged DNA ends that cannot be repaired, yielding an apoptotic signal. Overall, this cleavage has been named the "hallmark of apoptosis" (73).

Furthermore, activation of PARP-1 is also related to apoptosis-induced factor (AIF) dependent apoptosis, a process that is independent of caspases (74). Caspase independent apoptosis may occur in conjunction or before caspase-dependent apoptosis. PARP-1 stimulates the release of AIF from mitochondria where it is translocated to the nucleus to begin the alternative apoptotic pathway. Lastly, PARP-1 is cleaved by other proteases during apoptosis, but the mechanism and function are not fully understood.

Like PARP-1, PARP-2 has two caspase cleavage sites; caspase 3 and 8 cleave between the DNA binding domain and the catalytic domain, both yielding an inactive form of PARP-2 (22, 37, 75). The function of caspase mediated cleavage is similar to PARP-1 – a lack of DNA-dependent PAR activity will lock PARP-2 onto DNA ends allowing cells with irreparable damage to signal cell death. Furthermore, inhibiting PARylation will also allow

cells to restore both NAD^+ and ATP stocks (75). While caspase 3 cleaves PARP-1 and PARP-2, the selective interaction of caspase 7 with PARP-1, and caspase 8 with PARP-2, has not been fully defined.

IV. PARP Enzymology

Studying the kinetics of PARP enzymology proves difficult due to the unique enzymatic mechanism of the ART family. Unlike typical enzymes, which in the presence of a substrate, form an enzyme-substrate complex to then release the native enzyme and its enzymatic product, PARPs tend to enzymatically modify themselves. In addition, automodification may change the catalytic properties of the enzyme. Thus, in the presence of an allosteric activator and NAD^+, PARPs will bind NAD^+ creating the classic enzyme-substrate complex but during product formation, the enzyme-substrate complex becomes ADP-ribosylated (ES*) releasing nicotinamide.

Common Enzyme: $E + S \underset{k_{-1}}{\overset{k_1}{\leftrightarrow}} ES \overset{k_2}{\leftrightarrow} E + P$ **PARP Enzymes:** $E + S \overset{k_1}{\rightarrow} ES^*$

Due to the difficult enzymatic mechanism and no free product formation, studying PARP enzyme kinetics is challenging. Michaelis-Menten kinetics is the best equipped for PARP kinetics (7, 13, 76). In 1913, Leonor Michaelis and Maud Menten published their revolutionary work, "Die Kinetik der Invertinwirkung" (77). In this paper, Michaelis and Menten studied invertase, the enzyme that converts sucrose to fructose and glucose. In their study, Michaels-Menten kinetics relies upon the use of initial velocity to assume that measurements are taken when product formation is negligible and essentially zero. Once

initial velocity measurements were taken, Michaelis and Menten derived the following equations:

Michaelis-Menten Equations: $V_0 = \frac{V_{max}[S]}{K_M + [S]}$ $K_m = \frac{k_{-1} + k_2}{k_1}$ $V_{max} = k_2[E_{Total}]$

In the above equation, V_0 stands for initial velocity (rate) while V_{max} indicates the maximum velocity achievable by the system if saturating substrate concentrations are used; [S] represents the concentration of substrate. Lastly, the Michaelis-Menten constant, K_M, is defined as the substrate concentration at which 50% of V_{max} is achieved.

Importantly, there are a few assumptions built into the Michaelis-Menten model. First, as previously stated, initial rate measurements must be used in order to assume product formation is approximately equal to zero. Second, the binding step of E + S is fast while the catalysis of ES to E + P is slow yielding an equilibrium of [E], [S], and [ES]. Third, since [ES] is the measured component of Michaelis-Menten kinetics, it must be constant and at steady state. Fourth, the concentration of [S] must be much higher than [E] forcing [S] to be constant at early time points. Fifth and lastly, the enzyme must only exist in two forms, as free enzyme ([E]) and enzyme-substrate complex ([ES]).

PARP enzyme kinetics fits fairly well within Michaelis-Menten kinetics because it fulfills the second, third, and fifth assumptions listed above. With PARP-1 and PARP-2 preferentially modifying themselves, the enzyme-substrate complex of PARylated PARP will be a fast step and at steady state while the breakdown of PARylated PARP is incredibly slow and requires the addition of a glycohydrolase to digest PAR chains (assumption 2 and 3); therefore, the

PARP enzyme will only exist as unmodified and automodified PARP (assumption 5). The first and fourth assumptions are be met with proper enzymatic assay parameters.

Previous enzymatic assays include in gel using radioactive NAD^+ as a probe, ELISA-like assays, Western slot blot, or *in vivo* assays (7, 13, 57, 76), but all of these methods are limited in obtaining reliable kinetic data for purified PARP-1. Assays described in Beneke *et al*. (2010) and Clark *et al.* (2012) rely on the slot blot method in which PAR chains are cleaved from modified PARP-1 and hybridized to a membrane. After several wash steps, PAR chains are visualized through fluorescent antibodies. Langelier *et al*. (2010) established a colorimetric enzymatic assay for PARP-1 utilizing a histidine tag within PARP-1 to bind the protein to nickel coated plates. The addition of biotinylated NAD^+ with HRP-Streptavidin allowed visualization by plate reader at 450 nM and 550 nM.

Both of the listed methods rely upon multiple wash steps in addition to surface immobilization of PARP-1 in order to quantify the incorporation of PAR leading to increased error and potential loss of product. Overall, the two caveats to the methods may yield unreliable kinetic parameters. Moreover, the method applied by Langelier *et al*. require the addition of biotinylated NAD^+, which may not be utilized by PARP1 to the same degree as native NAD^+. Further, the use of non-native NAD^+ is not applicable to in solution and *in vivo* PARP kinetics. Similarly, the colorimetric method produced variable background results when negative control experiments (wells treated with only the washes) were performed (present work and data not shown) (78).

Optimizing an enzymatic assay with Abcam's NAD^+/NADH Assay kit eliminates the requirement of multiple washes and requires no new components for the modification reactions used in previous FRET, EMSA, or RAC assays (7, 29). Furthermore, the variable background readings experienced in the colorimetric method have been eliminated. Lastly and most importantly, a solution based enzymatic assay negates the concern of product loss through surface immobilization and subsequent wash steps. Using a fluorescence based enzymatic assay increases sensitivity, cohesiveness with other published methods, and provides consistent kinetic results.

V. Specific Aims & Goals

It is my goal in this study to define more clearly how PARP-1 and PARP-2 function within the nucleus in both the inactive and catalytically active states.

Through the development of a new fluorescent enzymatic activity assay, kinetic studies of PARP allosteric activation and relative binding affinities will provide clues into the nuclear function of PARP-1 and PARP-2 in regards to enzymatic activation and chromatin interactions. Due to its non-canonical DNA binding domain, PARP-2 may exhibit different preferences for enzymatic activators and therefore a function that is non-redundant with PARP-1. Likewise, the role of PARP-2 in chromatin dynamics and regulation is not known; therefore, the use of binding studies will provide a first glimpse into PARP-2 and chromatin interaction. Finally, many studies conclude the potential for PARP-1 and PARP-2 heterodimerization. Using relative binding affinity studies, limited proteolysis, and enzyme activity assays, the interaction, if any, between PARP-1 and PARP-2 will be characterized.

Here we report the first extensive and quantitative insight into PARP-1 and PARP-2 activators in addition to DNA-dependent activation. Further, we report the first solution based binding affinities for PARP-2. Overall, our data suggest that PARP-1 is activated strongly by DNA, including nucleosomes with DNA linker ends, as well as by its own enzymatic product, PAR. This indicates a mechanism by which PARP-1 might spread at sites of active transcription and DNA damage repair. PARP-2 is strongly activated by RNA and exhibits weak interaction with chromatin. This data suggests PARP-2 is not a chromatin associated PARP but may function in transcription during RNA synthesis and subsequent processing. Lastly, PARP-1 and PARP-2 are able to heterodimerize and elicit trans-activity indicating their role in a PAR mediated signaling cascade during DNA damage and transcription. Overall these data provide new insight into specificity and clarification for the roles of PARP-1 and PARP-2 during DNA damage and gene regulation.

METHODS & MATERIALS

Expression, fluorescent labeling, and automodification of PARP-1 and PARP-2

Expression and purification of PARP-1 and PARP-2

Human Poly-ADP Ribose Polymerase I (V762A), received from John Pascal (Thomas Jefferson University), and catalytically inactive mutant (E988K) were expressed and purified as previously described with a few modifications (78). The nickel-NTA purification was modified to an imidazole gradient from 20-400 mM imidazole; PARP-1 eluted between 115 to 210 mM imidazole. The gel filtration buffer increased from 150 to 500 mM NaCl to yield protein with higher purity and stability.

Human N-parp (residue 1-486, Figure 2A) was expressed and purified as published (7) with a few modifications. Nickel-NTA purification was modified from gravity flow to HPLC Nickel-NTA column. C-parp (residue 518-1014, Figure 2A) was purified as described for PARP-1; C-parp eluted from the Nickel-NTA column between 95-145 mM imidazole.

Mouse Poly-ADP Ribose Polymerase II, received from Dr. Michael Cohen (OHSU), and catalytically inactive mutant (E534A) were expressed as detailed (79). Purification of PARP-2 was followed as described (13). As with PARP-1, the salt concentration in the gel filtration buffer was increased to 500 mM NaCl.

Fluorescent labeling of PARP-1 and PARP-2

Purified PARP-1 (full length and truncations) and PARP-2 were labeled at their native cysteines with Alexa488 or Oregon Green 488, respectively (80). Equimolar amounts of PARP and fluorophores were mixed gently by rotating for 20 minutes at 4°C. Excess label was removed by buffer exchanging labeled PARP with 25 mM HEPES (pH 8.0), 0.1 mM EDTA, 500 mM NaCl, and 0.1 mM TCEP. Buffer exchange was done until the flow through was free of unbound label. A typical labeling efficiency was 65-85%. Stock aliquots (10µl) were frozen at -80°C for future use. Labeled protein was stable for a 4-5 days at 4°C.

Automodification of PARP-1 and PARP-2

Either labeled or unlabeled PARP-1 or PARP-2 (1 µM) was incubated in buffer containing 50 mM Tris-HCl (pH 8.0), 100 mM NaCl, and 1 mM $MgCl_2$. 53 base pair DNA (100 nM) and NAD^+ (600µM) was added and the reaction was incubated for 2 hours at room temperature. Automodification was stopped by adding a PARP inhibitor, PJ34 (1 mM final) and checked on a 4-12% denaturing gradient Criterion gel for 100% modification completion indicated by smearing on the gel. PARylation is a heterogeneous modification.

Purification of automodified PARP-1

PARP-1 (1µM) was incubated in the previously described activity buffer (50mM Tris-HCl, 100 mM NaCl, and 1mM $MgCl_2$) with 53 base pair 5'-biotinylated DNA (100 nM) and NAD^+ (600 µM) for 5 minutes, 2 hours, or overnight (7, 29). Each reaction was quenched with PJ34 (1mM final). Free biotinylated DNA and other reaction components were removed by purification over streptavidin coated Dynabeads. Excess NAD^+ and PJ34 were removed by

washing automodified PARP-1 with the gel filtration buffer, 25 mM HEPES (pH 8.0), 0.1 mM EDTA, 500 mM NaCl, and 0.1 mM TCEP. Purity was confirmed by 10% native TBE-PAGE and 8% denaturing SDS-PAGE.

Preparation of DNA and RNA oligomers

Annealing DNA and RNA oligomers

53 base pair DNA and RNA oligomers with the sequence 5'-ATC GGA CCC TAT ACG CGG CCG CCC TGG AGA ATC CCG GTG CCG AGG CCG CTC AA-3' and the addition of a 5'-phosphate, 5'-biotin, or 5'-Atto647 fluorophore were obtained from Integrated DNA Technologies (IDT). The reverse sequence of each DNA and RNA oligomer was used as a complement for annealing. Annealing was carried out by heating oligomers at 95°C for 5 minutes then the temperature decreased 0.1°C/second until held constant at 4°C. Annealing was checked on a 10% native TBE-PAGE.

Click chemistry to prepare circular DNA

A 53-bp oligomer, with the same sequence described above, was designed to contain a 5'-Hexynyl or 5'-Azide (IDT). The modified oligomer was annealed as described above to yield a double stranded product with 5' alkyne and 5' azide at both ends (Supplementary Figure 15A). The copper catalyzed cycloaddition reaction was performed in 100 mM NaCl, 10 mM Tris-HCl (pH 7.5), 0.2 mM EDTA and 1X phosphate buffered saline (PBS). 0.8 mM TCEP, 200 µM Tris[(1-benzyl-1*H*-1,2,3-triazol-4-yl)methyl]amine (TBTA), 0.8 mM $CuCl_2$ and 50-100 ng/µL DNA were added in that order to a low adhesion eppendorf tube (adapted from (79)). Due to the light sensitivity of TCEP, the reaction was protected from light and then

incubated at room temperature for 2 hours. The circular DNA was purified of reaction components using Zymo PCR Clean Up Kit. Efficiency of circular DNA was quantified by analytical ultracentrifugation and exonuclease treatment.

Linear or circularized DNA was treated with 1μL lambda exonuclease, a 5' exonuclease, for 30 minutes at 37°C. Reactions were run on a native 10% TBE-PAGE. Efficiency of the digestion was calculated by quantifying ratio of the 'cut' circular DNA to 'uncut' circular DNA. Typical efficiency of circularization was between 90-100%. The linear DNA was completely digested while the circularized DNA was not digested (Supplementary Figure 15B).

Octamer, dimer, and tetramer refolding and nucleosome reconstitution

Individual human or *Xenopus laevis* histones (H2A, H2B, H3.1, and H4) were denatured and refolded as described (81). Size exclusion chromatography yielded assembled dimer, tetramer, and octamer in 2 M NaCl. Mononucleosomes were assembled on 146 and 165 base pair DNA fragments derived from the '601' positioning sequence, as previously described (81). 146 base pair length represents minimal DNA length and no free DNA ends; 165 base pairs yield linker DNA arms of 7 and 11 base pairs. Trinucleosome constructs were assembled on 'non-linker ended' (NLE) and 'linker ended' (LE) trimer DNA, 561-bp and 621-bp, respectively (82). Complete saturation of assembly was confirmed by EcoR1 digestion and analytical ultracentrifugation.

Enzyme Assay

PARP (constant at 1 μM) and activators (nucleic acids, 100 nM; nucleosome or histones, 1 μM) were incubated together in 50 mM Tris-HCl (pH 8.0), 100 mM NaCl, and 1 mM $MgCl_2$ for 10 minutes at room temperature. Various concentrations of NAD^+ (2-75 μM) were added and the reaction was allowed to proceed for 45 seconds, a time point in which the velocity of modification was still linear and steady state (Figure 5C). Each reaction was quenched with PARP inhibitor, PJ34 (1 mM final). Unmodified PARP reactions were prepared by adding PJ34 prior to addition of activators and NAD^+.

Setting Up Modification Reactions (order of addition of reagents were as follows):
Inactive or Unmodified: PARP → PJ34 → Activator → 10 min → NAD^+
Active: PARP → Activator → 10 min → NAD^+ → 45s → PJ34

Quenched reactions were added in duplicate to a 384-well microplate. A standard curve was set up with serial dilutions of NAD^+ and added in duplicate to the microplate. To extract and quantify the amount of NAD^+ in solution, Abcam Fluorescent NAD^+ and NADH Assay kit (ab176723) was used according to the manufacturer's instructions, reducing the final volume to 18 μL. The microplate was scanned at a Typhoon imager, Ex/Em: 528/590 nM (Figure 5A).

Amount of NAD^+ in solution was quantified by ImageQuant software and reduced fluorescence of active PARP samples is indicative of NAD^+ incorporation and activation of PARP (Figure 5B). Quantified values were transformed from fluorescent signal into NAD^+ concentration in solution using the slope of the standard NAD^+ curve. Values were then corrected for NAD^+ incorporation by subtracting fluorescent readings of active samples from average fluorescence readings of inactive or unmodified samples. Initial rates (V_{max})

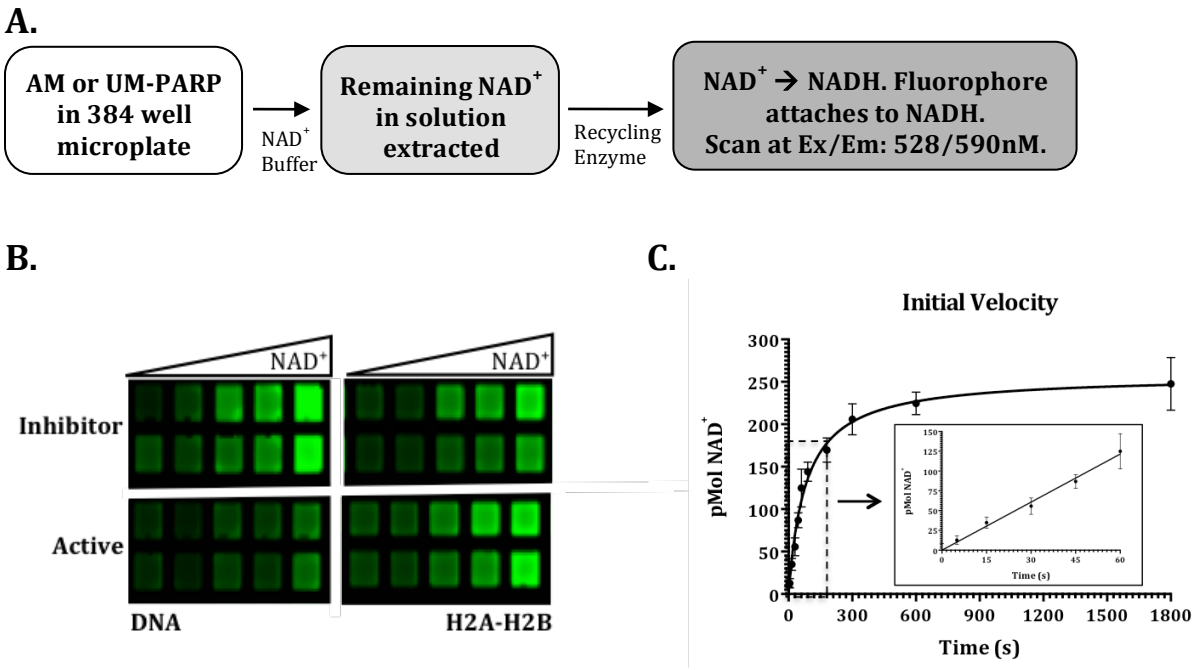

Figure 5: Introduction of the fluorescent enzymatic assay method.

- **A.** Schematic of the enzyme assay protocol. Quenched automodification reactions are added to a 384-well microplate and NAD^+ in solution is extracted with NAD^+ extraction buffer. Extraction is quenched with NADH extraction buffer. The recycling enzyme converts NAD^+ in solution to NADH; a fluorophore attaches to the converted NADH. The plate is scanned at Ex/Em: 528/590 nM.
- **B.** Representative microplate illustrating a decrease in fluorescence (NAD^+ in solution) in activated PARP (PJ34 added after activation with NAD^+) when compared to inhibited PARP (PARP-1+PJ34). Decrease of fluorescence is not seen with activators that do not stimulate PARP (e.g. H2A-H2B). NAD^+ titrated from 2-75µM.
- **C.** Initial velocity measure of PARP-1 and DNA over time. 45 seconds is in the linear portion of the graph therefore the system is under Michaelis-Menten conditions and used as the reaction time in the enzyme assay.

were plotted against NAD^+ concentration (S) and Michaelis-Menten curve parameters were calculated by Graphpad Prism using non-linear regression equation. Equations for calculating kinetic parameters can be found in Supplementary Figure 16.

HIFI-FRET Measurements

Affinity measurements were performed as detailed in (7, 29, 80). Atto-647N Maleimide (acceptor) labeled substrates were titrated against Alexa488 or Oregon Green 488 (donor) labeled PARP. Affinities were calculated using three different probe concentrations and fit with a quadratic equation for non-linear regression in GraphPad Prism to yield a global apparent K_D.

Job Plot Stoichiometry Measurements

Job plots were used to assign stoichiometries as described (29) using the continuous variation method (83). The initial titration step contained 100% nucleic acid or nucleosome followed by steps containing 25 nM increments and decreasing acceptor to keep the total concentration of the sample at 500 nM or 1 μM. The data was plotted FRET corrected data was plotted on Y-axis versus Molar Ratio (PARP: nucleic acid or nucleosome) on X-axis in GraphPad Prism. Curves were fit with various polynomial functions depending on the peak of the curve. The dash line drawn to the X-axis indicates the peak of the curve and the stoichiometric ratio.

Limited Proteolysis

20 μg of PARP-1, separately or in complex with PARP-2, were subjected to 1 μg trypsin (Roche Sequencing Grade) digestion with 10μL of each reaction being removed and quenched with 1 mM AEBSF at 0, 2, 5, and 15 minute time points. Each protein was digested individually as a reference control then FL-PARP-2 was mixed in equimolar amounts with PARP-1 (full length or truncated constructs). Quenched reactions were run on a denaturing 4-12% gradient Criterion gel and stained with Coomassie brilliant blue. Formation of protected bands indicates interaction of the two protein components and this interaction was confirmed by HIFI-FRET.

RESULTS

Poly (ADP-Ribose) Polymerase I and Poly (ADP-Ribose) Polymerase II specificity and function

Introduction

The ADP-Ribosyl Transferase (ART) family is composed of mono (ADP-ribose) transferases (MARTs) and poly (ADP-ribose) polymerases (PARPs) (4, 5). The most highly expressed and studied member of the ART family is PARP-1, a first responder to both DNA damage and active sites of gene expression. In its unmodified state, PARP-1 functions as a chromatin architectural protein by tightly binding and compacting chromatin (6, 10, 34, 35, 84). Upon sensing DNA damage or gene activation, PARP-1 catalyzes PAR chains onto itself and other proteins through auto- or hetero-modification, respectively. Catalytically active PARP-1 loses affinity for chromatin while gaining affinity for histones and nucleosome assembly activity (29).

The second most studied PARP, PARP-2, has a 69% structural homology (RMSD: 0.834) and a similar tertiary structure to the PARP-1 catalytic domain and is thought to be functionally redundant with PARP-1 in the nucleus (22, 37, 85). However, the N-terminal halves of the two proteins, responsible for DNA binding, are completely different. While PARP-1 has three canonical zinc fingers, PARP-2 has a basic alpha helical SAP domain, a non-canonical DNA binding motif. First discovered in a PARP-1 double knockout in mouse embryonic fibroblasts, PARP-2 exhibits only 5-10% of PARP activity in the cell but is surprisingly present in equal abundance to PARP-1 (18). One significant difference in the catalytic

domain is an insertion of 3 amino acids in a loop near the acceptor site and a narrower catalytic site in PARP-2 (14). The additional residues suggest potential specificity and individuality to activators of PARP-2 enzymatic activity.

Both PARP-1 and PARP-2 are activated are known to be activated in the presence of multiple DNA structures, RNA, histones and a variety of other nuclear factors (5-7, 13, 34, 46, 57, 86). However, studying PARP enzymatic kinetics proves challenging because PARPs do not follow a typical enzyme mechanism. To overcome this challenge, previous methods utilized non-native NAD^+, protein denaturation, surface immobilization, or protocols with multiple wash steps (13, 57, 76). These caveats made it difficult to distinguish the efficiency of various co-activators in stimulating PARP activity and thus make it difficult to separate potent activators from weak basal activators. Utilizing a fluorescence based assay, PARP is modified with native NAD^+ and quenched in solution by adding a potent PARP-1 inhibitor PJ34, thereby eliminating the need for denaturation. A fluorescent NAD^+/NADH assay is then followed to yield Michaelis-Menten kinetic parameters in response to various allosteric activators.

Here, we describe unique activators of both PARP-1 and PARP-2, indicating specific functions and mechanisms within the nucleus. PAR activates unmodified PARP-1 molecules both when it is in a free molecular form or covalently linked to PARP-1, providing a mechanism by which PARP-1 may spread at sites of active DNA repair and gene expression. Moreover, rather than being functionally redundant, RNA-dependent enzymatic activity of PARP-2 is greater than the stimulated activity of PARP-1, indicating a unique role of PARP-

2. Although structurally similar, PARP-1 and PARP-2 hold both redundant and distinct functions, specifically and in complex with one another, within the nucleus promoting the PARP family role in DNA damage and gene expression.

Results

Previously reported enzymatic activity and binding affinities utilized Sf9 insect cell expressed PARP-1 (7, 29). To increase yields and homogeneity, we switched to a bacterial (*E. coli*) expression system for PARP-1. Importantly, these results reported here are consistent with insect cell expressed PARP-1. HIFI-FRET affinity and stoichiometry measurements are within two-fold for DNA, dimer, tetramer, and nucleosome constructs while activity measurements are within three-fold difference (Supplementary Table 4). Thus, different expression systems do not affect measurements of affinity and activity and therefore, we utilize bacterially expressed PARP-1 for all experiments reported here.

PARP-1 predominately activates and binds to nucleic acids.

PARP-1 is activated by nucleic acids with a strong preference for double stranded DNA.

PARP-1 is a multi-domain protein with many known automodification sites (Figure 6A). Since PARP-1 is predominately known to activate in the presence of DNA damage, we first wanted to test nucleic acid dependent activation of PARP-1. To do this, identical blunt ended 53-base pair DNA (53DNA) sequences were designed with a 5' phosphate and 3' hydroxyl groups (Figure 6B). DNA with blunt ends has been previously shown to activate PARP-1 to a similar extent as 3' or 5' overhangs or nicked DNA. Furthermore, PARP-1 interacts with DNA through its 5' and 3' ends rather than on the sequence (7, 8, 13).

First, we wanted to quantify the dose-dependence of DNA dependent activation of PARP-1 in our assay. Using increasing concentrations of 53DNA (10-1000 nM), Michaelis-Menten parameters were calculated. DNA dependent activation is dose dependent, requiring at least 100 nM DNA per 1 μM PARP-1 to reach full activity and the activation rate remained within error at 1.57 μMol NAD^+ per minute per mg PARP-1 beyond 100 nM (Figure 7A). Importantly, trans-activation by mixing the DNA binding domain, N-parp (residues 1-486), and the catalytic domain, C-parp (518-1014), was not observed (Supplementary Figure 17) and was also seen in (7). PARP-1 must have a linker between the N-terminal and C-terminal domains in order to enzymatically activate.

Using 100 nM for all nucleic acid activators, PARP-1 activation was tested in the presence of DNA (singe stranded, ss and double stranded, ds), 'clicked' circular DNA (no free DNA ends), and no activator (Figure 7B). PARP-1 requires a full base pair, both a 3'-OH and 5'-PO_4^- ends, for activation indicated by lowered activation with single stranded DNA, 8-fold over basal (Figure 7B). The requirement of a full base pair supports previous studies stating the importance of two zinc fingers in DNA-dependent activation of PARP-1. To ensure that the preferable activation by single stranded nucleic acids was not a reflection of affinity towards these co-activators, we quantified the binding affinity for single stranded DNA with PARP-1 in which PARP-1 exhibited a weak affinity, >500 nM (Table 2).

Additionally, we wanted to test activation in the presence of no free DNA ends. We attached azide and alkyne groups to the ends of the 53bp DNA. During copper catalyzed

A.

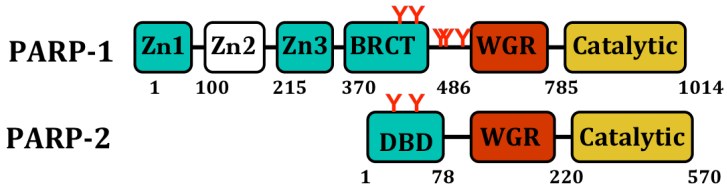

B.

5' – ATC GGA CCC TAT ACG CGG CCG CCC TGG AGA ATC CCG GTG CCG AGG CCG CTC AA – 3'	**53DNA (53bp)**
5' – CAG CGG AUA GGC – 3'	**12RNA (12bp)**
5' – AUC GGA CCC UAU ACG CGG CCG CCC UGG AGA AUC CCG GUG CCG AGG CCG CUC AA – 3'	**53RNA (53bp)**
5' – GGT GGC GGA CGT GTT TCA CGT ATA ATC GTG CGG GAC ACT GAC TCG TCA GTG CAT TGA GAA GGA GGA TAA AAT GCA CAT AGG TCG AAA GAC CTT ATA CAA GAA CTG TAT CAC CGG AGG GCG AGC ACC ACC – 3'	**129RNA (129bp)**

C.

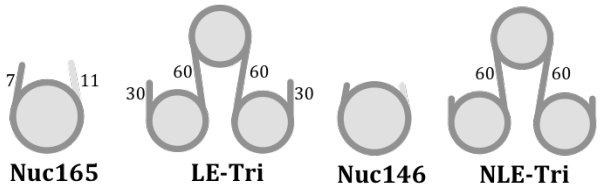

D.

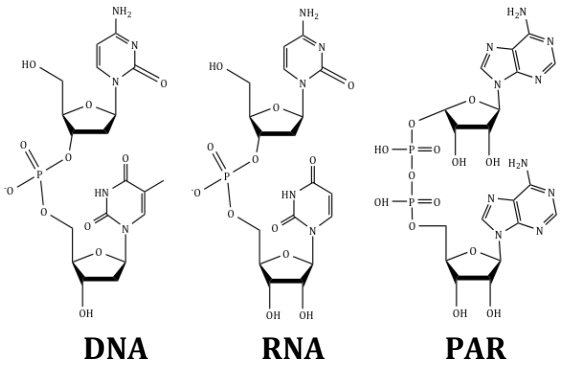

Figure 6: PARP domain structure and activators used in the enzyme assay.

- **A.** PARP-1 and PARP-2 are multi-domain proteins. Published automodification sites are labeled with a **Y**. PARP-1 is known to PARylate at D387, E488, and E491; PARP-2 is known to PARylate at K36 and K37.
- **B.** Sequence of the double stranded and single stranded nucleic acids used in the binding and enzyme assays. Sequences are identical between 53bp DNA and 53bp RNA. 12bp and 129bp RNA fragments were also tested.
- **C.** Cartoons of the nucleosome co-activators used in this assay. 165 mononucleosome (Nuc165) and linker-ended trinucleosomes (LE-Tri) have free DNA ends. 146 nucleosome (Nuc146) and non-linker ended trinucleosomes (NLE-Tri) have no free DNA ends.
- **D.** Cartoons of the nucleic acids used in the enzyme assay – only dinucleotides are shown. Structurally similar to DNA and RNA, PAR can be classified as a third type of nucleic acids.

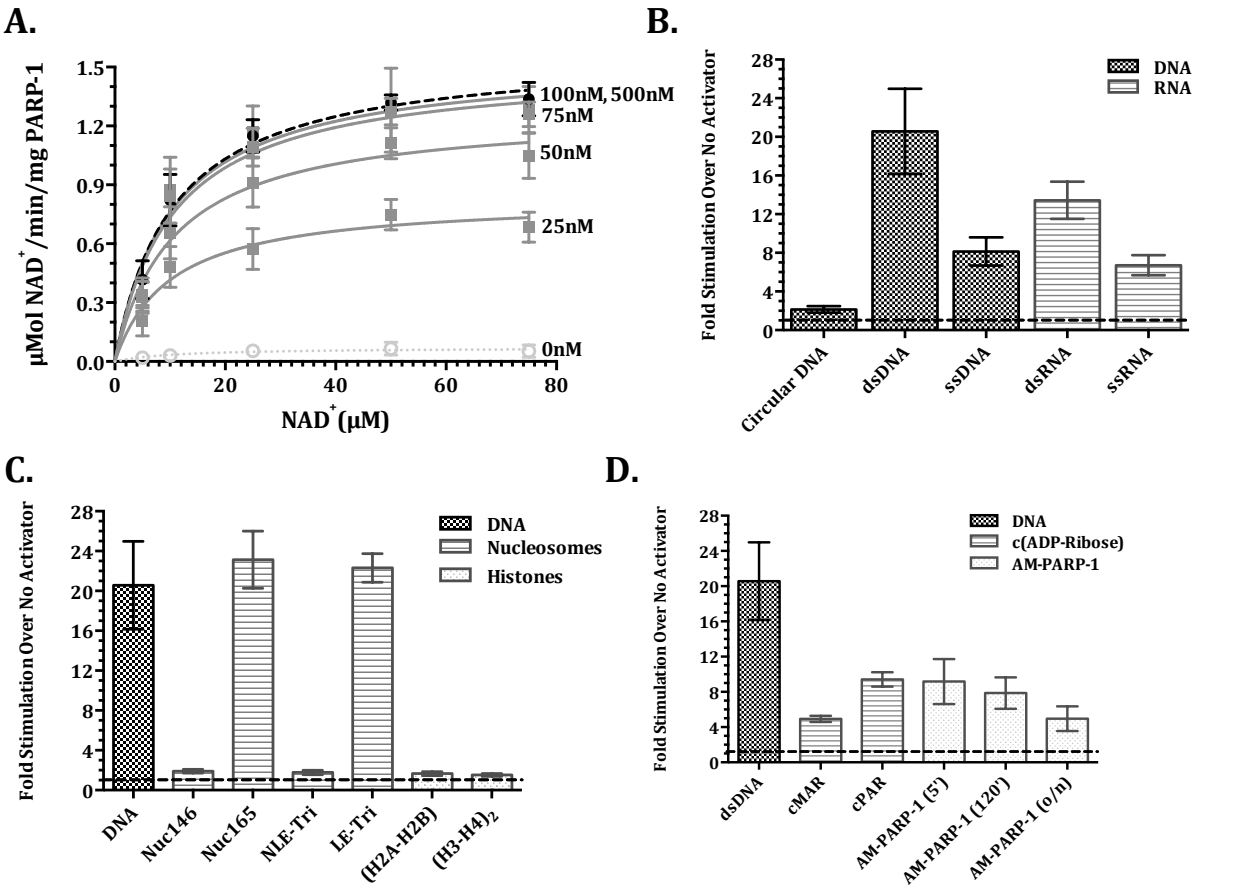

Figure 7: PARP-1 is preferentially activated by nucleic acids, including its enzymatic product, PAR.

- **A.** DNA-dependent activation of PARP-1 (1µM) is dose dependent with a minimum of 100 nM of DNA needed for full activation. For a complete list of parameters and concentrations, see Table 1.
- **B.** Bar graph quantifying V_{max} fold stimulation of DNA and RNA (1µM PARP-1, 100 nM activator, 45 s time point). Stimulation calculated as the ratio of activity measured in the presence and absence of activator. Dashed line indicates 1-fold stimulation. Error calculated from the standard deviation of three independent experiments. PARP-1 is activated by nucleic acids preferring double stranded substrates (a full base pair) to single stranded substrates. DNA activates PARP-1 to the greatest extent.
- **C.** Same as **B** for nucleosome and histone co-activators. Using DNA as the standard for comparison, PARP-1 is activated by nucleosomes with free DNA ends to a greater level compared with free DNA. PARP-1 only showed basal activity in the presence of Nuc146 and NLE-Tri nucleosomes and histone complexes.
- **D.** Same as **B** for commercial ADP-Ribose and automodified PARP-1. PARP-1 is activated in the presence of cPAR and *in vitro* AM-PARP-1.

cycloaddition, reduced copper will catalyze a 1,2,3 triazole linkage between the azide and alkyne groups (Supplementary 15A and B) (87). This linkage creates a bond that is nearly impossible to reduce or oxidize thus ensuring no DNA ends will be present in the sample. In the presence of 100 nM 'clicked' circularized DNA, PARP-1 activation is similar to its basal levels. Clicked DNA only exhibited 2-fold stimulation over background (Figure 7B). This level of activation remained constant even when clicked DNA concentration was increased to 500 nM (data not shown).

Next, we wanted to quantify RNA-dependent activation of PARP-1 utilizing three single stranded RNA constructs and one double stranded RNA construct (Figure 6B). PARP-1 prefers DNA to RNA, with 21-fold and 13-fold stimulation over basal levels, respectively (Figure 7B). The preference of DNA and RNA is because of a decrease in V_{max} (μMol NAD^+/min/mg PARP) from 1.57 to 1.02 and not K_M, which is within error (Table 1). Thus, this difference is due to the presence of the activator rather than changes in affinity of PARP-1 for NAD^+. To explore if this enzymatic preference was due to affinity of PARP-1 for the activator, we next determined the dissociation constant of unmodified Alexa-488 labeled PARP-1 with Atto-647 labeled double and single stranded DNA and RNA using HIFI-FRET. FRET can be used to measure interaction between two binding partners due to the strong distance dependence between acceptor (Atto-647) and donor (Alexa-488) fluorophores. PARP-1 binds dsDNA and dsRNA with a strong affinity, 6.8 nM and a 5.8 nM, respectively (Table 2). Thus the difference in PARP-1 activity is not due to affinity. Importantly, the enzymatic activity is carried out at activator concentrations well above the

K_D meaning the affinity of PARP-1 for the activator should not be a factor in enzymatic simulation.

We next performed Job plot analyses to determine stoichiometries for PARP-1 binding to DNA and RNA. As expected from the crystal structure (8), PARP-1 has only one binding site for DNA. This is illustrated by a peak at 0.66, indicative of 1 PARP-1 molecule per DNA end (or 2 PARP-1 to every 1 DNA molecule). In contrast, the peak shifts to 0.5 with RNA indicating a 1:1 PARP-1 to RNA complex. The difference in stoichiometry of PARP-1 with DNA or RNA is likely due to the secondary structure of RNA yielding only 1 RNA end available for PARP-1 binding. To confirm that the activation preference between DNA and RNA was not due to affinity and stoichiometry differences, even though the enzyme assay is performed at concentrations above the K_D, RNA concentration was increased to 500 nM and the maximum activation (V_{max}) remained within error. Similarly, like ssDNA, PARP-1 prefers double stranded nucleic acids exhibited by only a 6-fold stimulation of ssRNA over basal activity for 3 single stranded constructs (12RNA, 53RNA, and 129RNA; Supplementary Figure 15C) as well as a weak binding affinity >500 nM (Table 1 and 2).

Overall, these results suggest that PARP-1 activation is primarily mediated by interaction with DNA ends but PARP-1 is also be activated by RNA. Activation is dependent upon free 5' and 3' ends and importantly, a full base pair.

Histones and nucleosomes without linker DNA do not activate PARP-1.

Previous studies reported that PARP-1 was potently activated by nucleosomes (7, 49, 86). We tested PARP-1 activation by nucleosomes and trinucleosomes with and without free linker ends (29). We assembled a single nucleosome on the '601' positioning sequence with two different lengths of DNA, 146 and 165 base pairs. The 146 mononucleosome (Nuc146) has no linker DNA arms while the 165 mononucleosome (Nuc165) has two free DNA linker arms, 7bp and 11bp (Figure 5C). Representing higher order chromatin structures, we assembled three nucleosomes on the '601' positioning sequence. The Non-Linker Ended Trinucleosomes (NLE-Tri) have 60 base pairs of DNA connecting the central nucleosome to the two adjacent nucleosomes, but no free DNA ends. The Linker-Ended Trinucleosomes (LE-Tri) have two 30bp arms extending from each flanking nucleosome in addition to the 60 base pair links (Figure 5C).

PARP-1 was tested in the presence of all four nucleosome constructs for enzymatic activation with the concentration of nucleosomes held at 1μM, equimolar to PARP-1, to ensure any activation of PARP-1 by nucleosomes would be seen and due to known stoichiometry of PARP-1 towards these substrates (29). The two nucleosomes with extranucleosomal DNA linkers (Nuc165 and LE-Tri) activate PARP-1 to a level similar to DNA, both mononucleosomes and tri-nucleosomes exhibited 23-fold and 22-fold stimulation over basal activity, respectively; similar to what was observed with free DNA (Figure 7C). Removal of free DNA linker arms in Nuc146 and NLE-Tri reduced PARP-1 activation to only 3-fold stimulation over basal activity. This is despite the fact that PARP-1 binds NLE-Tri with an affinity of 4.8 nM (29). Interestingly, the catalytic efficiency ($s^{-1}M^{-1}$),

the ratio of k_{cat} (s^{-1}) over K_M (M), for PARP-1 increased in the presence of nucleosomes compared to free DNA (Table 1). With free blunt ended DNA, PARP-1 has a catalytic efficiency of $18.6x10^4$ $s^{-1}M^{-1}$ and with LE-Tri, PARP catalytic efficiency increases to $25.0x10^4$ $s^{-1}M^{-1}$ (Table 1). This increase is due to an increase in V_{max} rather than decrease in K_m. In the presence of trinucleosomes, PARP-1 has a maximum velocity of 1.7 μMol/min/mg PARP-1 while in the presence of free DNA, velocity drops to 1.57 μMol/min/mg; however, the K_M remains within error (Table 1). This phenomenon is also exhibited in the presence of mononucleosomes with linker ends (Table 1). PARP-1 enzymatic activity in the presence of mononucleosomes and trinucleosomes is not affected by a 10-fold difference in affinity, 2.2 nM and 12.7 nM, respectively (7, 29). From the catalytic efficiency calculations, we conclude that PARP-1 is activated slightly more efficiently in the presence of linker-ended nucleosomes than free DNA.

With numerous studies reporting activation of PARP-1 by histones (5, 6, 86), we then tested both individual histones and histone complexes for PARP-1 enzymatic activation. Recombinant human histones and histone complexes were reconstituted by salt dialysis and purified by size exclusion chromatography to yield pure protein/complexes. We only used histones where the 260/280 ratio was below 0.6, to ensure that there was no DNA contamination (a common problem for many histone preparations). The four individual histones (data not shown), refolded H2A-H2B dimer, and $(H3\text{-}H4)_2$ tetramer only activate PARP-1 at most 2-fold over basal activity (Figure 7C). This is supported by the weak affinity of unmodified PARP-1 for histone complexes, >500 nM (29).

Together, these results indicate PARP-1 activation in a chromatin context is due to blunt ended DNA linker arms, rather than through interaction with histones and/or histone tails. Moreover, the restricted movement or geometry of DNA linker arms in the context of a nucleosome or nucleosomal array resulted in higher catalytic efficiency of PARP-1 with linker-ended nucleosomes in comparison with free DNA. Overall, these data illustrate the preference of PARP-1 for DNA ends, whether it is protein-free or wrapped in a nucleosome.

Poly-ADP ribose and automodified PARP-1 activates unmodified PARP-1.

The product of PARP-1 enzymatic activation, PAR, is often referred to as the third type of nucleic acid due to its structural similarity to both DNA and RNA. In addition, PAR has twice the negative charge per monomeric unit (48) (Figure 5D). Since PAR is similar to both nucleic acids that have been shown to activate PARP-1, we tested whether PARP-1 is also activated by PAR. We first used commercial PAR (cPAR, Trevigen) and mono (ADP ribose) (cMAR, Sigma Aldrich) at a final concentration of 100 nM. Unexpectedly, both mono and poly (ADP-ribose) activate PARP-1. cMAR and cPAR activate PARP-1 with a 5-fold and 9-fold stimulation over basal activity, respectively (Figure 7D). However, due to the heterogeneity of PAR, we do not have a technique to calculate the length of the PAR chains tested here.

Because the vast majority of free PAR chains are attached to a protein, free cMAR and cPAR are not necessarily biologically relevant. We therefore wanted to test whether PARP-1 was activated by automodified PARP-1. We incubated PARP-1 in the presence of biotinylated DNA and NAD^+ for 5 min, 120 min, or overnight, to be used as activators for unmodified

PARP-1. Quenching and purifying the reaction is crucial to ensure that the only activity recorded is from unmodified PARP-1 and not a continuing modification from these reactions. The purified AM-PARP-1 reactions (at 100 nM initial PARP-1 concentration) were then tested as potential activators of unmodified PARP-1. Both AM-PARP-1 modified for 5 min and 120 min activated PARP-1 to a similar extent to what was seen with cPAR, 9-fold and 8-fold over basal activity, respectively (Figure 7D). However, when modification was increased to overnight incubation, fold stimulation drops to 5. Notably, the K_M and catalytic efficiency increase and decrease, respectively, between commercial PAR and AM-PARP-1, which is most likely due to the heterogeneous nature of PAR (Table 1). Together, our data identify PAR, both free and covalently linked, as a novel and potent activator of PARP-1 enzymatic activity.

PARP-2 exhibits unique enzymatic activity and affinity in comparison with PARP-1.

PARP-2 is preferentially activated by RNA to a similar extent as PARP-1.

Unlike PARP-1, PARP-2 contains a non-canonical DNA binding domain and exhibits a significantly lower enzymatic activity overall. Due to the weaker enzymatic activity and efficiency of PARP-2 and the non-canonical DNA binding domain of PARP-2, we tested and compared PARP-2 enzymatic activation in response to various nucleic acid activators tested for PARP-1. We first compared DNA dependent activation of PARP-1 and PARP-2 under identical conditions, and found that PARP-2 is 4.4 times less active than PARP-1 (Figure 8A and B, Table 1). This difference in catalytic activity is likely due to a difference in K_M; PARP-1 has a K_M of 15.9 μM while PARP-2 is 3-fold weaker at 41 μM (Table 1). The difference in both k_{cat} and K_M becomes more apparent in the specificity constant (k_{cat}/K_M)

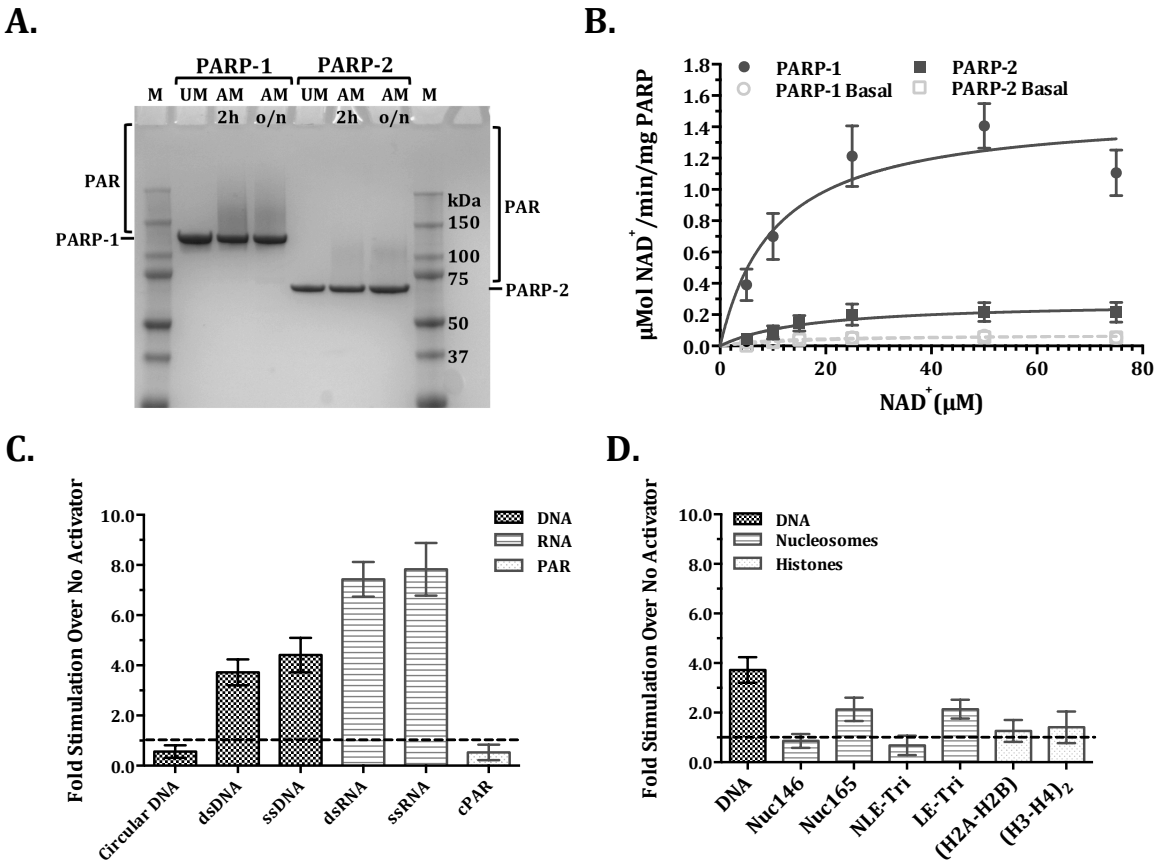

Figure 8: PARP-2 is strongly activated by RNA, to a similar extent as PARP-.1

- **A.** Automodification reactions of PARP-1 and PARP-2. M, molecular weight marker; UM: inhibited reactions; AM: automodified reactions with DNA and NAD^+. Reactions were set up for two time points 2 hours (2h) and overnight (O/N). PAR is a heterogenous modification causing smearing on gel. Lower activation of PARP-2 exhibited by less smearing in both time points.
- **B.** Quantified Michaelis-Menten parameters for DNA dependent activation of PARP-1 and PARP-2 with basal activity of PARP-1 (blue, dashed line) and PARP-2 (green, dashed line). V_{max}, µMol NAD^+/min/mg PARP, plotted against varying substrate, NAD^+ (µM), concentration.
- **C.** Same as **1B** for PARP-2 and nucleic acids. PARP-2 preferentially activates in the presence of RNA.
- **D.** Same as **1B** for PARP-1 and nucleosome activation. PARP-2 prefers free DNA and doesn't activate well with nucleosomes or histones.

in which PARP-1 and PARP-2 show close to a 20-fold difference, $18.6x10^4$ and $0.92x10^4$ $s^{-1}M^{-1}$ (Table 1). This striking difference in catalytic specificity led us to test other nucleic acid activators – PARP-2 may exhibit preference for another allosteric activator aside from DNA.

Unexpectedly, PARP-2 showed a strong preference for RNA-dependent activation in comparison to DNA. In the presence of DNA, PARP-2 has a maximum velocity of 0.356 μMol/min/mg while in the presence of RNA, PARP-2 velocity increases 2-fold (Figure 8C, Table 1). Surprisingly, the activation of PARP-2 in the presence of RNA is almost the same as that of PARP-1, an apparent V_{max} of 0.711 for PARP-2 and 1.02 μMol/min/mg for PARP-1. Thus, while PARP-2 is less active in the presence of DNA, the preferred PARP-1 activator, RNA stimulates PARP-2 to levels exhibited by PARP-1. In addition, unlike PARP-1, PARP-2 shows a slight preference for single stranded DNA and RNA, 4 and 8-fold stimulation over no activator (Figure 8C). In fact, PARP-2 is stimulated to a similar or even greater extent by single stranded nucleic acids when compared with PARP-1. The V_{max} of single stranded nucleic acids with PARP-1 is 0.620 μMol/min/mg and 0.512 μMol/min/mg for DNA and RNA, respectively (Table 1). In the presence of PARP-2, single stranded nucleic acid dependent velocity increases to 0.422uMol/min/mg and 0.749uMol/min/mg (Table 1). This stimulation is so great that ssRNA is the only activator in which PARP-2 almost overcomes the higher K_M to activate to a similar level as PARP-1. The catalytic efficiency of PARP-1 and PARP-2 for ssDNA is only a 3-fold difference compared with a 20-fold efficiency difference in dsDNA-dependent activation (Table 1). Importantly, the significant enzymatic activation was also exhibited by 12bp and 129bp ssRNA fragments, with kinetic

data within error of 53bp ssRNA data reported here (Table 1). Lastly, like PARP-1, PARP-2 requires a free DNA end, which is seen in lack of activation in the presence of circular DNA (Figure 8C). Overall, these data show that unlike PARP-1, PARP-2 prefers RNA over DNA, stimulating to higher levels than seen with PARP-1 when single stranded RNA is present.

The striking difference in PARP-1 and PARP-2 activation led us to question whether such a difference was due to a difference in the affinity for various nucleic acid substrates. Employing HIFI-FRET to determine the distance between donor labeled PARP-2 and acceptor labeled Atto-647 DNA and RNA, binding affinities (K_D^{app}) are reported here. In comparison with PARP-1 (6.8 nM and 5.8 nM), PARP-2 exhibits an 8-fold weaker affinity for DNA and RNA, 56.6 nM and 48.1 nM respectively.

Using Job plot measurements, we found that one PARP-2 molecule binds two DNA molecules. In contrast, the stoichiometry of PARP-2 shifts in the presence of double stranded RNA. Using RNA with an identical sequence to the previously quantified DNA molecule, we found three PARP-2 molecules binds two double stranded RNA molecules (Table 3). These stoichiometries suggest self-association behavior of PARP-2 or multiple binding sites for nucleic acids on a single PARP-2 molecule, most likely due to its non-canonical N-terminus. Similar to PARP-1, which does not bind to single stranded nucleic acids, PARP-2 also exhibits >500 nM affinities for ssDNA and ssRNA (Table 2). Although PARP-2 has drastically weaker affinities, about 10-fold, than PARP-1, both are predominately stimulated by nucleic acids. Overall, PARP-2 preferentially activates with RNA rather than DNA.

Due to the similarities in enzymatic preference for PARP-1 and PARP-2 with nucleic acids, we expected PARP-2 to be activated in the presence of PAR, although most likely to a lesser extent because of the lack of 5' phosphate. Surprisingly, PARP-2 cannot be activated in the presence of 100 nM cPAR (Figure 8C); increasing concentration of PAR to 500 nM did not significantly change enzymatic stimulation (data not shown).

Together, these data illustrate that while PARP-2 is considered to hold redundant functions, PARP-2 differs in its nucleic acid affinity and activity, likely due to the non-canonical DNA binding domain. First, PARP-2 holds a slight preference for single stranded over double stranded nucleic acids and is activated to a greater extent than what was measured for PARP-1 using our sensitive enzymatic assay. Second, PARP-2 is strongly activated in the presence of RNA with a catalytic efficiency similar to PARP-1.

PARP-2 activates to a greater extent with free DNA than with nucleosomes.

Although PARP-2 has a lower activation rate than PARP-1 for nucleic acids, we wondered if PARP-2 would be activated in the presence of nucleosomes and histone complexes. We used all co-activators tested for PARP-1 activity. Similarly to PARP-1, PARP-2 was not activated in the presence of non-linker ended nucleosomes (Nuc146 and NLE-Tri). PARP-2 exhibits only <1-fold stimulation over basal activity when no free DNA arms are present (Figure 8D). Similarly, histone dimer and tetramer do not activate PARP-2 beyond basal levels, with only 1-fold stimulation (Figure 8D). Like PARP-1, PARP-2 enzymatic activity is stimulated by linker-ended nucleosomes, 2-fold stimulation for Nuc165 and LE-Tri (Figure 8D). However, these stimulation levels are lower than that seen with free DNA, 3.7-fold

over basal (Figure 8C). Thus, unlike PARP-1, PARP-2 shows almost a 2-fold preference for free DNA compared to nucleosomal DNA. This preference is exhibited in the $V_{max,}$ decreasing from 0.356 to 0.204 μMol/min/mg for DNA and LE-Tri, but not K_M, which remains within error (Table 1). This fold decrease is also seen with Nuc165 (Table 1). Therefore, the activator difference is purely due to free DNA versus nucleosomal DNA rather than variation of K_M. Moreover, these changes cause a two-fold difference in catalytic efficiency, 0.92 $s^{-1}M^{-1}$ and 0.56 $s^{-1}M^{-1}$ for Nuc165 and LE-Tri.

This result led us to test affinities of PARP-2 with nucleosomes by HIFI-FRET. Atto-647 labeled Nuc146 and Nuc165, were titrated against constant Oregon Green-488 labeled PARP-2. Similar to PARP-1, PARP-2 binds weakly to Nuc146 as quantified with a K_D^{app} greater than 1000 nM (Figure 9A, Table 1). However with the addition of linker arms in Nuc165, the affinity increased to 92.8 nM, over 40-fold weaker than that of PARP-1 (Figure 9A, Table 1). Likewise and contrary to PARP-1, the affinity of PARP-2 for Nuc165 is 2-fold weaker than the affinity of PARP-2 for free DNA.

Due to the difference in stoichiometry between PARP-1 and PARP-2 for free DNA, we tested the stoichiometry of PARP-2 with mononucleosomes. PARP-2 exhibits the same stoichiometry as PARP-1 in the presence of Nuc165 forming a 1 to 1 complex (Figure 9C, Table 3). The 1 to 1 ratio is reinforced by the nucleosome having two linker DNA arms, so the stoichiometry would be 1 PARP-2 molecule per 2 DNA linker arms; the same stoichiometry recorded for free DNA.

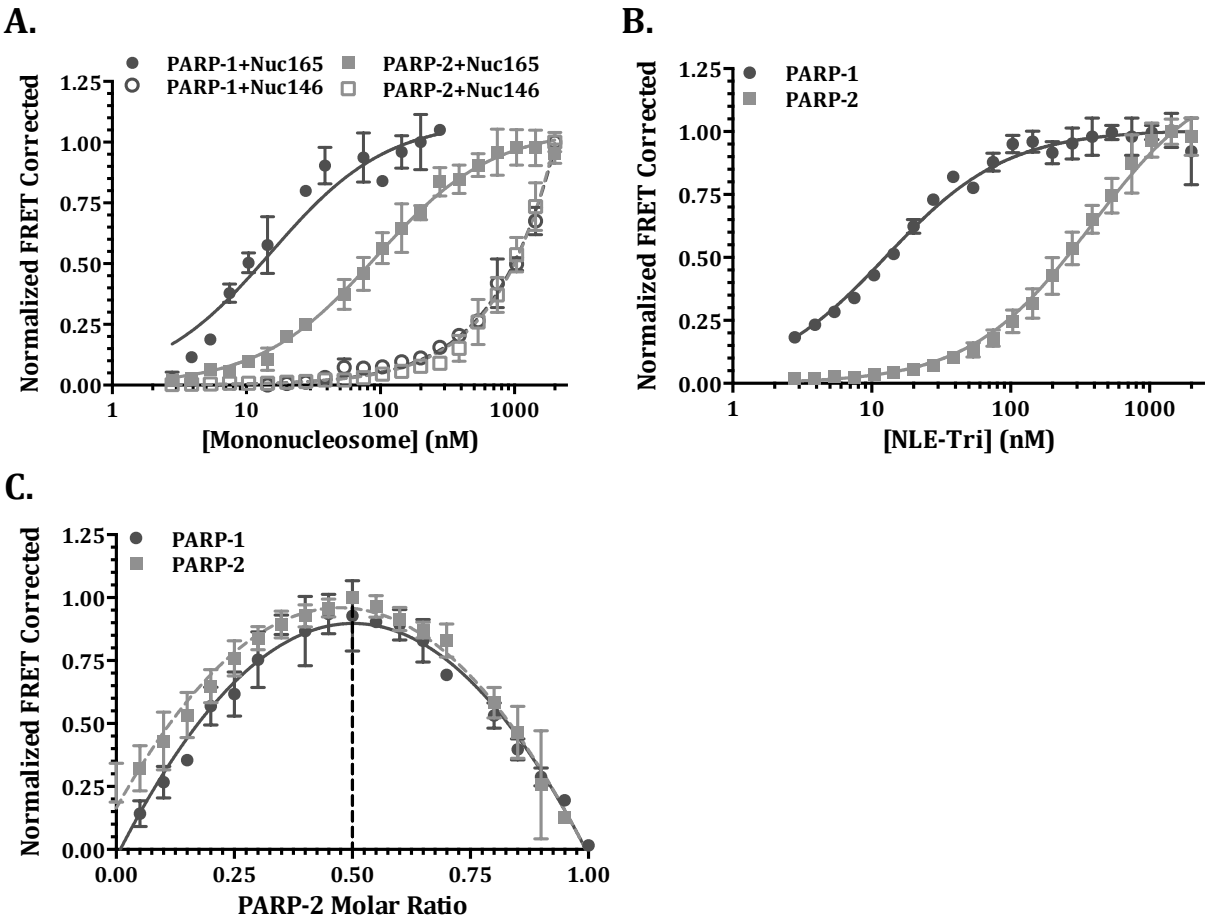

Figure 9: PARP-2 interacts weakly with both DNA damaged and native chromatin.

- **A.** Binding curves of PARP-1 and PARP-2 to Nuc165 and Nuc147. PARP-1 data from Clark *et al*, 2012. JBC. PARP-1 donor concentrations were kept constant at 5 nM for Nuc146 and at 1, 2, and 3 nM for Nuc165.
- **B.** Binding curves of PARP-1 and PARP-2 to NLE-trinucleosomes. PARP donor concentrations were kept constant at 2 or 3 nM.
- **C.** Stoichiometry measurement of PARP-1 and PARP-2 to Nuc165 determined by Job plot. The dashed lines indicate the peak of the curve and the stoichiometry.

In light of the weaker affinity of PARP-2 for mononucleosomes with free linker DNA, damaged chromatin, we tested the binding affinity of PARP-2 for non-linker ended tri-nucleosomes (NLE-Tri), non-damaged native chromatin. Previously it was shown, PARP-1, while not binding to mononucleosomes in absence of linker DNA, binds NLE-Tri with high affinity (7, 29). Similar to PARP-2 binding mononucleosomes with a weaker affinity than PARP-1, PARP-2 binds NLE-Tri with significantly weaker affinity, 381.6±14.2nM (Table 2). Thus, unlike the two distinct modes of PARP-1 binding chromatin, PARP-2 exhibits weaker affinity with both modes of chromatin, damaged and non-damaged chromatin. Overall these activity and affinity data reinforce the idea of PARP-2 having distinct functions independent of PARP-1 redundancy in the cell. PARP-1 remains the prominent chromatin related PARP protein in the nucleus; PARP-2 exhibits weaker affinity and activation with mononucleosomes and higher-order chromatin, tri-nucleosomes.

PARP-1 and PARP-2 hetero-dimerize with each other and stimulate enzymatic activity

PARP-1 AND PARP-2 form a low nanomolar affinity complex.

Several studies in literature report the ability of PARP-1 and PARP-2 to heterodimerize and trans-activate each other using methods like GST-tagged pull downs (62, 88). To confirm and quantify these findings in solution, we sought out to quantify the dissociation constant of this PARP-1/PARP-2 interaction by HIFI-FRET. Atto647N acceptor labeled PARP-2 was titrated against Alexa488 labeled PARP-1 to yield a low nanomolar binding affinity of 63 nM (Figure 10A, Table 2). To narrow down the binding interface of PARP-1 and PARP-2,

A.

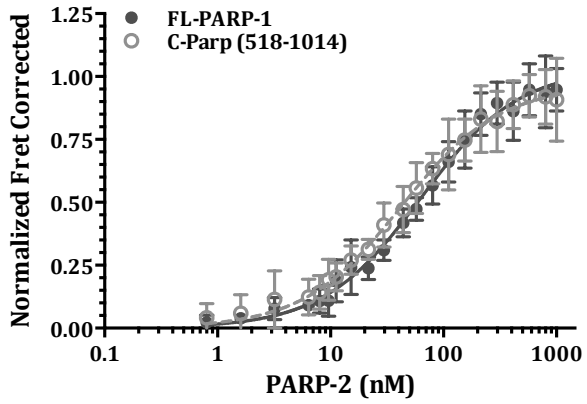

B.

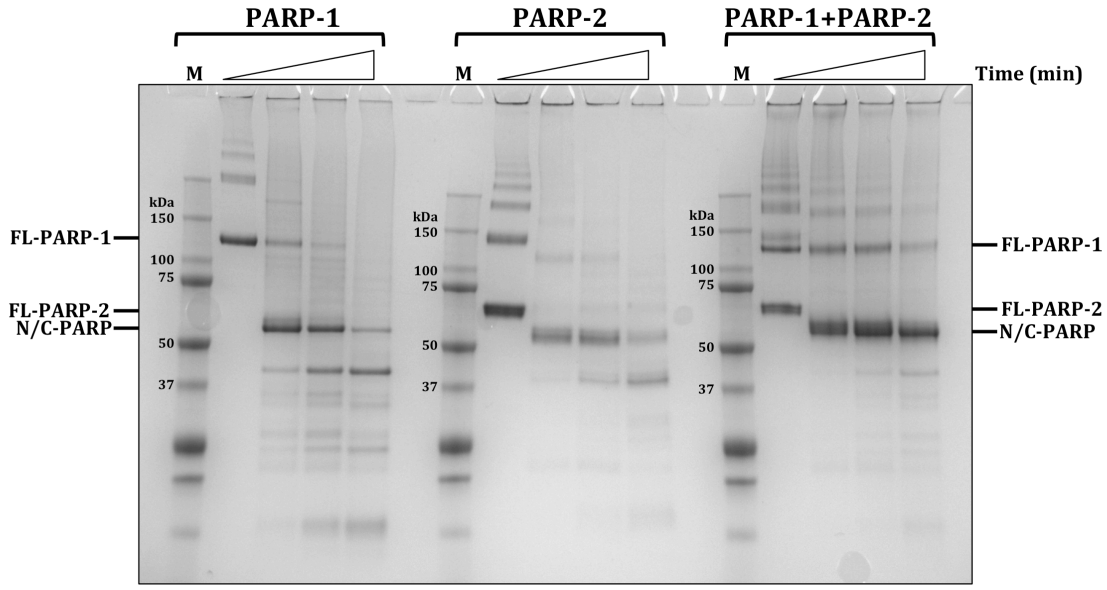

Figure 10: PARP-1 and PARP-2 form a low nanomolar complex.

- **A.** Binding curve of full length PARP-1 and C-parp with PARP-2. PARP-1 donor concentrations were held constant at 2 and 4 nM.
- **B.** Limited proteolysis of PARP-1 and PARP-2 with trypsin. Time points were taken at 0, 2, 5, and 15 minutes. Molecular weights in kDa listed next to molecular weight marker lanes (M). Both FL-PARP-1 and a 50kDa band is protected when PARP-1 and PARP-2 are mixed which indicates interaction. Banding above the full-length proteins is due to the excess protease inhibitor, AEBSF, used to quench the reaction.

we tested donor labeled Alexa488 DNA binding, N-parp (1-486) and the catalytic half, C-parp (518-1014). PARP-2 binds the catalytic domain of PARP-1 with a stronger affinity than even full length PARP-1, 43 nM (Figure 10A, Table 2). No FRET signal was reported for N-parp and PARP-2 so other methods will be needed to confirm any potential interaction.

Next, we performed limited proteolysis of the PARP-1 and PARP-2 complex with trypsin to confirm the FRET results and use another method in attempt to narrow down the potential binding interface. Surprisingly, a 50kDa fragment, not seen in PARP-1 and PARP-2 alone proteolysis, was protected when PARP-1 and PARP-2 bind. Additionally, FL-PARP-1 was also protected. Trypsin cleaves PARP-1 between N-PARP-1 and C-PARP-1 (7); thus, this 50kDa fragment was most likely the N-terminus of PARP-1 or C-terminus of PARP-1 or PARP-2 (Figure 10B). Further mass spectrometry experiments will be carried out to identify the protected fragments to determine the exact interaction interface.

PARP-1 and PARP-2 activate one another in trans.

Because of the tight binding affinities of PARP-1 and PARP-2, we wanted to see if PARP-1 and PARP-2 could activate each other. To do this, catalytically inactive point mutants, PARP-1 E988K and PARP-2 E534A, were expressed and purified (13). To ensure inactivity, we quantified the binding affinity of both mutants to H2A-H2B dimer under automodification conditions (Figure 11A). Catalytically active PARP-1 and PARP-2 exhibit low nanomolar affinities for histones when automodified, 2.3 nM and 10.5 nM, respectively (29) (Figure 11B, Table 2). However, both point mutants exhibited only very low levels of interaction, >500 nM. Further, in the presence of DNA and NAD^+, neither mutant protein

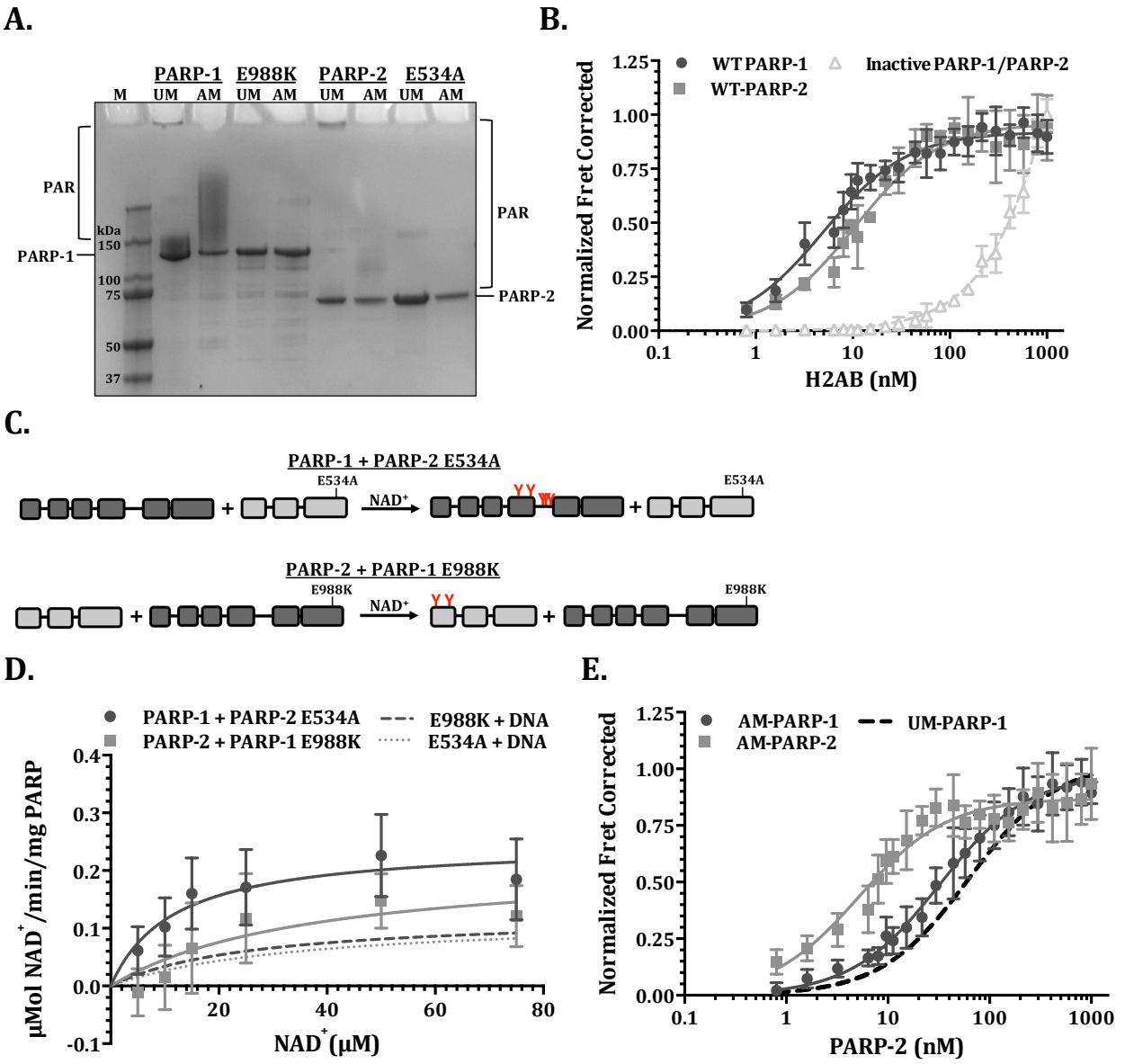

Figure 11: PARP-1 and PARP-2 form a trans-activating heterodimer.

- **A.** Automodification reactions of wild type and catalytically inactive PARP-1 (E988K) and PARP-2 (E534A). M, molecular weight marker; UM: inhibited reactions; AM: automodified reactions with DNA and NAD^+. PAR is a heterogenous modification causing smearing on gel. No smearing with point mutants indicative of no activation.
- **B.** Binding curve of PARP-1, PARP-2, and catalytically inactive point mutants with (H2A-H2B). In the presence of DNA and NAD^+, PARP-1 and PARP-2 bind H2A-H2B with low nanomolar affinity but when inactive, PARP-1 and PARP-2 loses ability to bind histones, indicative of lack of automodification.
- **C.** Michaelis-Menten curve for PARP-1 and PARP-2 trans-activity. Point mutant activation with DNA shown in dashed lines.
- **D.** Binding curve of AM-PARP-1, AM-PARP-2 and UM-PARP-1 (non-linear line of best fit) with UM-PARP-2.

shows any PAR formation, as demonstrated by lack of smearing in a denaturing gel. Importantly, neither protein exhibited DNA-dependent activity in the enzymatic assay; any recorded stimulation recorded was within error with basal levels.

Next, we tested trans-activity of PARP-1 and PARP-2. Using PARP-1 E988K and PARP-2 E534A as activators for PARP-2 and PARP-1, respectively, for the enzymatic assay, we quantified Michaelis-Menten kinetic parameters (Figure 11C). Surprisingly, PARP-1 and PARP-2 both stimulate some level of activity in one another, 3 and 2-fold over basal stimulation respectively (Figure 11D, Table 1). Notably, this is the first quantitative evidence indicating that PARP-1 and PARP-2 elicit trans-activation.

Due to both the tight binding affinity and enzymatic activation of PARP-2 by PARP-1 (and vice versa) we wanted to test whether automodification of PARP-1 affected its affinity. Alexa488 labeled PARP-1 was modified in the presence of DNA (100 nM) and NAD- (600 μM) for two hours at room temperature (Figure 11A). Atto647-PARP-2 was then titrated against AM-PARP-1. Surprisingly, automodification increases the binding affinity of PARP-2 to PARP-1 by two-fold to 32.1 nM (Figure 11E, Table 2). Next, to confirm if the affinity of PARP-2 is PARP-1 specific, we automodified Oregon Green 488 PARP-2 and tested FRET in a similar manner (Figure 11A). Unexpectedly, while PARP-2 cannot bind unmodified PARP-2, at least in the scope of FRET, the affinity of unmodified PARP-2 for AM-PARP-2 is 5.2 nM (Figure 11E, Table 2). Thus PARP-2 binds unmodified PARP-1 and both automodified PARPs with high affinity. The interaction of PARP-2 with automodified substrates could be

due to conformational changes induced by PARylation or through direct interaction with the PAR chains.

Overall the data presented herein indicate PARP-1 and PARP-2 specificity within the nucleus, as well as in conjunction as a trans-activating complex. Using DNA as the standard of comparison for all other activators, PARP-1 is preferentially activated in the presence of double stranded DNA and nucleosomes with free DNA ends (Figure 12A, left panel). PARP-2, on the other hand, is preferentially activated by both single and double stranded RNA (Figure 12A, right panel). Although PARP-1 and PARP-2 have very different affinities for NAD^+, as reflected in K_M (Figure 12B), PARP-2 activates to a similar extent as PARP-1 in the presence of RNA (Figure 12C, Table 1). PARP-2 binds much weaker to nuclear components, most surprisingly, to chromatin both with and without linker DNA ends. Further, another striking difference is the lack of PAR mediated activation for PARP-2 while PARP-1 exhibits strong PAR activation. Lastly, PARP-1 and PARP-2 form a functional complex capable of trans-activation.

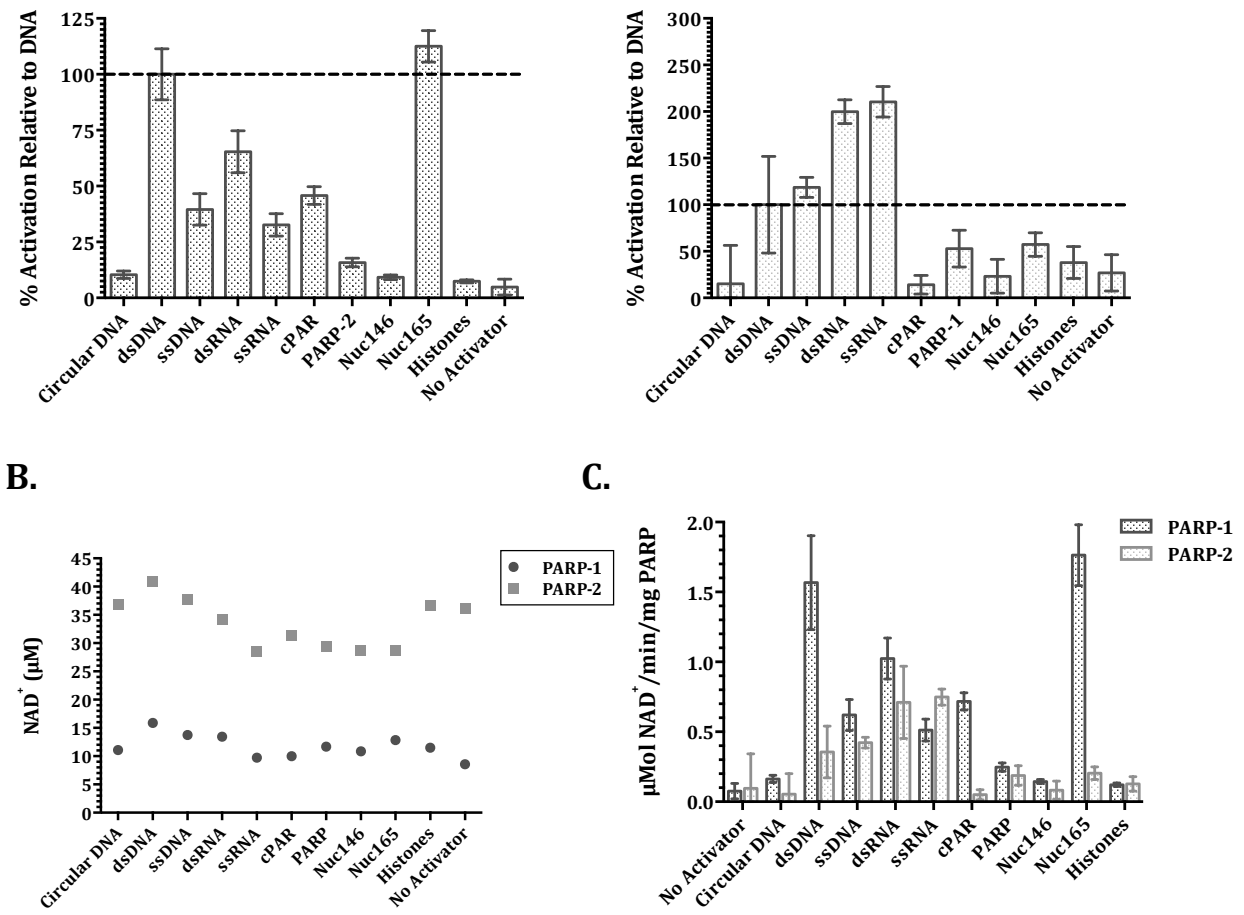

Figure 12: Overview of enzymatic properties of PARP-1 and PARP-2

- **A.** Overview of PARP-1 (*left panel*) and PARP-2 (*right panel*) activation in relation to DNA. Michaelis-Menten kinetic parameters of PARP-1 and PARP-2 are shown in Table 1. The V_{max} for each activator was divided by the V_{max} for DNA to yield a percent stimulation in comparison with DNA-dependent activation. The dashed line indicates DNA at 100% activation; DNA served as a reference for other allosteric activators.
- **B.** Average K_m, affinity for NAD^+, values for PARP-1 and PARP-2 activators. PARP-1 exhibits a lower Km and thus higher affinity for NAD^+ when compared to PARP-2, over all activators tested.
- **C.** Bar graph comparing the apparent V_{max} for PARP-1 and PARP-2 in the presence of various allosteric activators. All activators tested under identical conditions.

Table 1: Enzymatic parameters for PARP-1 and PARP-2

Reaction conditions were as follows: 50mM Tris (pH 7.5), 100mM NaCl, 1mM $MgCl_2$. K_D^{app} values taken from Table 2.
Final Concentrations: PARP-1, 1μM; Nucleic acids, 100nM; Chromatin and Histones, 1μM.

Allosteric activators	PARP-1					PARP-2				
	$K_D^{(app)}$ *(nM)*	V_{max} *(μmol/min/mg)*	K_m *(μM)*	k_{cat} *(s^{-1})*	k_{cat}/K_m *($s^{-1}M^{-1}$)*	$K_D^{(app)}$ *(nM)*	V_{max} *(μmol/min/mg)*	K_m *(μM)*	k_{cat} *(s^{-1})*	k_{cat}/K_m *($s^{-1}M^{-1}$)*
Basal Activity		0.076±0.05	8.55	0.14	$1.68x10^4$		0.055±0.01	36.13	0.06	$0.31x10^4$
Nucleic Acids										
Circular DNA		0.163±0.03	11.08	0.31	$2.77x10^4$		0.053±0.14	36.77	0.06	$0.16x10^4$
dsDNA (53bp)	6.8±0.4	1.57±0.34	15.9	2.95	$18.6x10^4$	56.6±3.1	0.356±0.19	40.98	0.38	$0.93x10^4$
ssDNA (53bp)	>500	0.620±0.11	13.73	1.17	$8.51x10^4$	>500	0.422±0.04	37.80	0.34	$0.91x10^4$
dsRNA (53bp)	5.8±0.4	1.02±0.15	13.44	1.93	$14.4x10^4$	48.1±2.8	0.711±0.26	34.19	0.76	$2.21x10^4$
ssRNA (53bp)	>500	0.512±0.08	8.72	0.97	$9.93x10^4$	>500	0.749±0.06	28.59	0.80	$2.79x10^4$
ssRNA (12bp)		0.532±0.05	11.47	1.00	$8.74x10^4$		0.790±0.1	32.37	0.80	$2.60x10^4$
ssRNA (129bp)		0.646±0.08	11.54	1.22	$10.4x10^4$		0.756±0.1	36.48	0.8	$2.20x10^4$
Histones										
(H2A-H2B)	>500[2]	0.127±0.02	11.5	0.24	$2.07x10^4$	>500	0.121±0.04	34.53	0.13	$0.37x10^4$
$(H3-H4)_2$	>500[2]	0.116±0.01	10.00	0.22	$2.19x10^4$	>500	0.135±0.06	36.65	0.14	$0.39x10^4$
Chromatin										
Nuc146	>500[1]	0.145±0.01	10.43	0.27	$2.61x10^4$	>500	0.083±0.06	37.39	0.09	$0.24x10^4$
Nuc165	2.2±1.5[1]	1.76±0.22	15.93	3.32	$20.9x10^4$	92.8±4.2	0.204±0.05	38.78	0.22	$0.56x10^4$
NLE Tri	4.8±2.1[2]	0.14±0.02	10.85	0.26	$2.36x10^4$	381.6±14.2	0.065±0.04	38.70	0.07	$0.20x10^4$
LE-Tri	12.7±6.7[2]	1.70±0.11	12.83	3.20	$25.0x10^4$		0.206±0.05	34.15	0.22	$0.56x10^4$
ADP-Ribose										
cMAR		0.376±0.03	10.00	0.71	$7.08x10^4$					
cPaR		0.718±0.06	9.75	1.73	$17.7x10^4$		0.050±0.04	31.39	0.05	$0.17x10^4$
AM-PARP-1 (5')		0.699±0.20	16.77	1.32	$7.85x10^4$					
AM-PARP-1 (120')		0.600±0.14	18.63	1.13	$6.07x10^4$					
AM-PARP-1 (ON')		0.378±0.11	13.26	0.71	$5.38x10^4$					
FL-PARP										
PARP-1/PARP-2	63.0±3.0	0.248±0.03	11.69	0.47	$4.00x10^4$	63.0±3.0	0.219±0.08	37.7	0.2	0.68x104

[1] Clark et al, 2012. JBC [2] Muthurajan et al, 2014. PNAS.

Table 2: Apparent binding affinities for PARP-1 and PARP-2

Reaction Conditions: 25mM Tris (pH 7.5), 200mM NaCl, 0.01% NP-40, 0.01% CHAPS**.** Error from standard deviation of 3 individual experiments performed in duplicate.

Binding Substrate	PARP-1		PARP-2	
	K_D^{app} *(nM)*	R^2	K_D^{app} *(nM)*	R^2
Nucleic Acids				
dsDNA	6.8±0.4	0.9	56.6	0.98
ssDNA	>500		>500	0.98
dsRNA	5.8±0.4	0.9	48.1	0.98
ssRNA	>500		>500	0.97
Histones/Chromatin				
(H2A-H2B)	>500	0.93	>500	0.98
NLE-Tri	4.8±2.1[1]	0.86	381.6±14.2	0.98
PARP				
UM-PARP-1			63.0±3.1	0.95
C-PARP-1			42.0±2.5	0.93
N-PARP-1			--	--
AM-PARP-1			32.1±1.8	0.93
UM-PARP-2			--	--
AM-PARP-2			5.2±0.4	0.89

Table 3: Job plot stoichiometries for PARP-1 and PARP-2

Reaction Conditions: 25mM Tris (pH 7.5), 200mM NaCl, 0.01% NP-40, 0.01% CHAPS**.** Error and R^2 from the standard deviation of 3 individual experiments performed in duplicate. Stoichiometry ratios represented PARP to substrates**.**

Binding Substrate	PARP-1		PARP-2	
	Stoich.	R^2	Stoich.	R^2
Nucleic Acids				
dsDNA	2 to 1	0.93	1 to 2	0.97
dsRNA	1 to 1	0.93	3 to 2	0.95
Chromatin				
Nuc165	1 to 1	0.95	1 to 1	0.93
NLE-Tri	1 to 1			

DISCUSSION

Development of the enzymatic assay

The enzymatic assay employed in this study provides a means to accurately measure native enzymatic activity of PARPs in solution. Eliminating surface immobilization and use of non-native NAD^+ analogs, the enzymatic activity reported here can be compared to PARP kinetics *in vivo*. Particularly in the case of PARP-1, the automodification sites on the protein are expansive and not fully characterized, thus immobilization could limit automodification potential and moreover, limit activity-induced protein conformation changes. Next, the use of wash steps and/or cleavage of PAR chains inherently yield error within an assay; these caveats are removed by keeping PARP proteins in the PARylated form as well as by excluding wash steps.

The assay reliably and quantitatively allows us to calculate reproducible enzymatic parameters for two different PARP proteins under identical conditions, in the presence of a variety of activators. First PARP proteins are automodified in solution with NAD^+ utilizing buffers similar to those in previous experiments. This way, results can be directly compared to previous methods using automodified PARP-1 (e.g. FRET, EMSA, nucleosome assembly assays) (7, 29). Next, automodified PARP is added to treated 384-well microplates (80) and remaining NAD^+ in solution is quantified using Abcam's Fluorescent NAD^+/NADH Assay Kit. Originally designed to quantify NAD^+ and NADH in cellular extracts, this kit can be used for *in vitro* PARP kinetics if proper controls are put into place. The pitfalls of this assay are in relying on NAD^+ in solution and the need to calculate NAD^+ incorporation. Thus, calculating less active or lowered activity for PARP proteins

introduces error and difficulty during quantification. Nonetheless, even with these limitations, it is still a big improvement over previously published assays. All of the DNA results recorded herein are with two to three fold of previous *in vitro* enzymatic studies for PARP-1 and PARP-2 (7, 13, 78). Notably, the values presented here are two or three fold *above* the previously described slot blot western that requires cleavage of PAR chains and wash steps, and thus loss of kinetic data and lower activation reported. Likewise, the values presented here are two or three fold *below* the previously described colorimetric assay that yielded high background and false positives, thus an over-estimation of kinetic data and high activation recorded.

PARP-1 & PARP-2 nucleic acid interaction and activation

Studied primarily through DNA damage, both PARP-1 and PARP-2 are known to bind and be activated in the presence of various forms of DNA (7, 13). From the crystal structure, we know that PARP-1 requires a full base pair for interaction via PARP-1 zinc fingers. Zn1 and Zn2 are required for binding while Zn3 is required for DNA-dependent activation (8). Nonetheless, PARP-1 binds and is activated in the presence of many DNA structures including gaps and overhangs (7, 13). PARP-2, on the other hand, only requires a 5' phosphate for DNA-dependent activation and requires flaps or gaps for DNA binding (13, 63). PARP-1 and PARP-2 are known to have distinct roles in DNA damage and repair; PARP-1 signals DNA damage to repair proteins while PARP-2 participates in the ligation of DNA strands.

Here, we further elucidate the interaction of PARP-1 and PARP-2 with single and double stranded DNA. Confirming previous results (7, 13, 78), PARP-1 prefers a full base pair of DNA for binding and activation, single stranded reagents showed less activation and much weaker binding. Interestingly, PARP-2 is activated by both single-stranded and double-stranded DNA but only binds double stranded DNA weakly. The primary difference in the DNA-dependent activation of PARP-1 and PARP-2 is in the activation of PARP-2 with single stranded DNA. The difference in activation between PARP1 and PARP-2 for single stranded DNA is reinforced by the previously discussed binding modes (Figure 4). In complex with DNA, PARP-2 requires a full double helix for all activation dependent residues to form contacts with the DNA, removing a strand would lessen the residue contacts of Zn3 with the DNA backbone. PARP-2, on the other hand, only requires one side of the DNA backbone to come in contact with the WGR in order to activate fully. Thus, PARP-1 would have weaker activation with single stranded reagents while PARP-2 may not differentiate.

This suggests PARP-2 may participate in DNA ligation, DNA replication, and recombination where single stranded DNA intermediates are prevalent. Interestingly, though, the interaction of PARP-2 with single stranded DNA is purely transient and not due to PARP-2 tightly binding single stranded DNA to form a complex. PARP-1, in contrast, primarily interacts with double stranded DNA, which it would encounter in nicked chromatin and DNA damage.

Recently, PARP-1 and PARP-2 have been implicated in regulating RNA synthesis and processing. Both proteins are able to activate in the presence of ribosomal RNA; however,

the activation of PARP-2 is much stronger (5, 57). Nonetheless, the studies of PARP-1 and PARP-2 with RNA in terms of affinity and activity are extremely limited and purely qualitative. Here, we provide the first quantitation of PARP-1 and PARP-2 activity and affinity with single (three different constructs, Supplementary Figure 15C) and double stranded RNA. PARP-1 interacts with RNA in a similar manner to DNA due to the respective activation and affinities of PARP-1 for DNA and RNA. The slight difference in activity and stoichiometry between DNA and RNA could be due to the multiple conformational states of RNA in solution – RNA is more flexible and adopts different structures aside from the double helix similar to DNA. Importantly, PARP-1 activity remained within error regardless of predicted secondary structure for each single stranded RNA sequence tested reinforcing the importance of the nucleic acid structure rather than sequence.

Surprisingly, and unlike PARP-1, PARP-2 preferentially is activated in the presence of RNA rather than DNA; but like PARP-1, PARP-2 exhibits similar affinities for DNA and RNA. The stimulated activity of PARP-2 with single and double stranded RNA illustrates the only activators in which PARP-2 almost overcomes weaker enzymatic efficiency to activate to similar extent as PARP-1. Similar to PARP-1, PARP-2 activity remained stable when testing various RNA sequences and predicted folding (Supplementary Figure 15C). Thus, this result highlights a striking difference between PARP-1 and PARP-2. Although PARP-2 is a much weaker enzyme, the preferred activator of PARP-2 is RNA rather than DNA, a result previously described by Leger *et al*, though in a qualitative manner (57). This preference could be due to the difference in N-terminal domain or conformational folding of PARP-1

and PARP-2 as it is unclear where RNA would interact with PARP-2, though it has previously been suggested to bind the DNA binding SAP domain in the N-terminus.

Overall, PARP-1 and PARP-2 function with nucleic acids in the nucleus. These data suggest roles for the proteins in a variety of processes from DNA replication and recombination to DNA damage repair. Notably, PARP-2 may hold a specific role during RNA synthesis and processing. PARP-1 has been implicated in alternative splicing, but there is no evidence for the role of PARP-2 in the process. The roles of PARP proteins in RNA synthesis and processing need to be further explored.

PAR mediated activation of PARP-1 & PARP-2

Several studies speculate an interaction of PARP-1 with PAR as a possible mechanism of spreading of PARP-1 and PAR at sites of active gene expression, as seen in *Drosophila* heat shock genes (45, 46). Additionally, PAR has a chemically similar to DNA and RNA (48, 89).

In the enzymatic activity, only PARP-1 is activated by PAR, both in its free form and covalently linked to PARP-1. Stimulation of PARP-1 by PAR provides a possible mechanism for PARP-1 spreading at DNA damage and gene expression. DNA damage or transcriptional triggers stimulate initial activation of PARP-1, while downstream activation might be due to the subsequent PARylation of adjacent chromatin-bound PARP-1 molecules.

Free and covalently linked PAR activates PARP-1 but not PARP-2. The difference in PAR activation of PARP-1 and PARP-2 could be due to protein conformation and/or PAR

interactions with PARP-1 through its N-terminus, a region that is not homologous to the PARP-2 N-terminus. Nevertheless, while PARP-2 cannot activate in the presence of PAR, it may interact with PAR chains. Through FRET experiments, we found when PARP-2 is automodified, unmodified PARP-2 binds with low nanomolar affinity. AM-PARP-2 binding could be due to a conformational change in the PARP-2 molecule induced by activation or direct interaction with PAR chains, an interaction that doesn't yield enzymatic activation.

Overall, these data points toward functional specificity for PARP-1 and PARP-2 in the nucleus. First, PARP-1 activity is stimulated in the presence of its own enzymatic product, PAR. Prior to PAR functioning as a negative feedback inhibitor of PARP-1 activity (3, 34), PAR, strikingly, may activate neighboring PARP-1 molecules. Thus, in addition to PARP-1 serving two distinct functions as a chromatin architectural protein and a histone chaperone, PAR similarly holds two distinct functions. PAR initially stimulates PARP-1 activity prior to acting as a negative regulator of PARP-1 activity. Secondly, PARP-2 may not be activated by PAR, but can bind PARylated PARPs and possibly PAR chains, an indicated by a strong interaction of PARP-2 with PARylated PARP-1 and PARP-2. However, it is most likely that the PARylation of PARP-1 and PARP-2 causes a conformational change allowing the binding site of PARP-2 to become more accessible rather than a direct interaction with PAR. The potential binding of PARP-2 to PARylated PARP or PAR suggests a potential mechanism for recruitment of PARP-2 to sites of transcription and damage (21, 56).

PARP-1 & PARP-2 chromatin interaction

PARP-1 has also been studied in its role as a chromatin architectural protein that is able to bind and thereby compact chromatin. The binding of chromatin by PARP-1 has been reinforced with various studies utilizing solution-state binding affinity measurements, AFM, and AUC (7, 29, 35, 90). Due to the non-canonical DNA binding domain, we expected PARP-2 to have a very different interaction with chromatin when compared to PARP-1. While PARP-1 shows no preference between free DNA and nucleosomal DNA, in binding and enzymatic activity, PARP-2 both binds and is activated to a lesser extent if nucleosomes are present.

The weaker nature of PARP-2 and chromatin interaction is true for both previously characterized modes of PARP-1 binding (7, 29). First, PARP-2 will bind free DNA linker-ended nucleosomes, but with much weaker affinities than seen with free DNA or reported for PARP-1. Secondly, PARP-2 binds non-linker ended trinucleosomes but with an affinity that is over 80-fold weaker than that of PARP-1. Further, PARP-2 does not activate as efficiently in the presence of nucleosomes compared to free DNA; the lowered activation is most likely due to a starkly different N-terminus of PARP-2. Alternatively, it could be due to the conformation change of PARP-2 when it binds the nucleosomes or steric hindrance of the nucleosome blocking the limited DNA ends.

Overall, the affinity and activity studies show that PARP-2 may not be a chromatin interacting PARP and thus, PARP-1 remains the prominent chromatin related PARP in the nucleus. The PARP-1 chromatin interaction is enzymatically independent and dependent

serving as a chromatin architectural protein and a histone chaperone, respectively. PARP-2, on the other hand, interacts only weakly with chromatin *in vitro*, and thus may rely on additional mechanisms for chromatin interactions *in vivo*. Additionally, PARP-2 chromatin interactions reported here only concern major-type histones rather than centromeric chromatin. Previously published studies have suggested that histone variants or additional post-translational modifications of histones are required for chromatin binding (21, 39, 56). Therefore, PARP-2 may have functions that were not explored here.

PARP-1 & PARP-2 functional interaction

PARP-1 and PARP-2 function within the nucleus as individual proteins to interact with DNA damage and gene expression. Although PARP-1 and PARP-2 have been speculated to homodimerize through the helical subdomain in the catalytic terminal, we have not been able to reproduce this by analytical ultracentrifugation (AUC) and size exclusion chromatography coupled with multi-angle light scattering (SEC-MALS). Thus, the heterodimerization of PARP-1 and PARP-2 was unexpected. The affinity of PARP-1 for PARP-2 is in the low nanomolar range and the affinity increases by 2-fold when only the catalytic terminal domain of PARP-1 is tested. This suggests that PARP-2 interacts with PARP-1 via the C-terminus (WGR, HD, and ART subdomains) and moreover, the N-terminus provides either steric hindrance or repulsion of PARP-2 due to the lower affinity of the full-length protein – at least in the scope of experiments performed here. Notably, the affinity of PARP-2 to C-parp is the strongest observed affinity for PARP-2 indicating PARP-2 binds with low nanomolar affinity to DNA, RNA, and PARP-1. Similar to automodified PARP-2,

automodified PARP-1 also binds PARP-2 with even tighter affinity that was seen with C-parp, although a significantly weaker, about 5-fold, affinity than AM-PARP-2.

The quantification of a binding affinity between PARP-1 and PARP-2 provides the first quantitative evidence of heterodimeric complex formation. Further, PARP-2 interacts with the catalytic half of PARP-1, the termini consisting of the helical domain and the ADP-ribosyl transferase domain. Past studies imply the helical domain (HD) may also serve as the homodimerization domain; therefore, it is likely the HD domain may serve as a heterodimization domain for PARP-1 and PARP-2. Interestingly, PARP-2 interacts even stronger when the protein is automodified. The PARylation effect may be due to direct interaction with PAR or conformational changes in the protein due to activation. The activation induced conformational changes could allow for greater accessibility of the catalytic domains of PARP-1. In general, PARylation incites a mode of PARP-2 binding activity, a phenomenon previously uncharacterized.

In addition to forming a heterocomplex , PARP-1 and PARP-2 also trans-activate each other; PARP-1 and PARP-2 serve as novel enzymatic activators of one another. The binding and subsequent activation of PARP-1 and PARP-2 may provide a mechanism to prolong PARylation at sites of DNA damage and transcription. PARP-2 PARylation, while it is slower to accumulate, is much longer-lived than PARP-1 transient PARylation in vivo (37). Stabilizing PARylation at DNA damage and transcription would allow for these processes to be completed accurately and without error while providing other repair factors an opportunity to perform their functions.

Overall the data presented herein provide clarification and characterization of the two prominent nuclear PARPs, PARP-1 and PARP-2. Both proteins function individually as responders to DNA damage and regulators of gene expression while also forming a trans-activating complex. By functioning individually and as a complex, this study indicates PARP-1 and PARP-2 in a complex PAR independent and dependent signaling cascade (Figure 13).

First, in its unmodified state, PARP-1 binds chromatin as an architectural protein thereby condensing chromatin. Upon DNA damage or transcriptional signals, PARP-1 will bind DNA and automodify. The automodification is triggered most likely by DNA and linker nucleosomal DNA. Once automodified, PAR covalently linked to PARP-1 triggers automodification of downstream PARP-1 molecules to yield a widespread signal for DNA damage or active gene expression. Both unmodified and automodified PARP-1 signal the recruitment of unmodified PARP-2 molecules to these sites. Once recruited, PARP-2 can bind automodified PARP-2 to form an additional dimeric complex and further the recruitment of PARP-2 molecules.

Once recruited, PARP-2 may also be PARylated at lysine 33 and 37 to help influence chromatin dynamics or recruit other factors. Activation and subsequent automodification of PARP-2 is stimulated by single stranded nucleic acids, most prominently, single stranded RNA. Once activation, PARP-2 may stabilize PAR chains at these sites due to its slower accumulation and NAD^+ turnover as well as through the recruitment of other unmodified PARP-2 molecules. Further, AM-PARP-2 may trigger additional PARP-1 automodification

via the PAR chains. Additionally, an unmodified PARP-1 and PARP-2 heterodimer stimulates trans-activation, although it is unclear which PARP protein is being PARylated. The signaling cascade continues until DNA damage is repaired or transcription is complete. Once complete, poly-glycohydrolases (PARGs) digest PAR chains to release the modifications allowing PARP-1 and PARP-2 to return to their inactive native states.

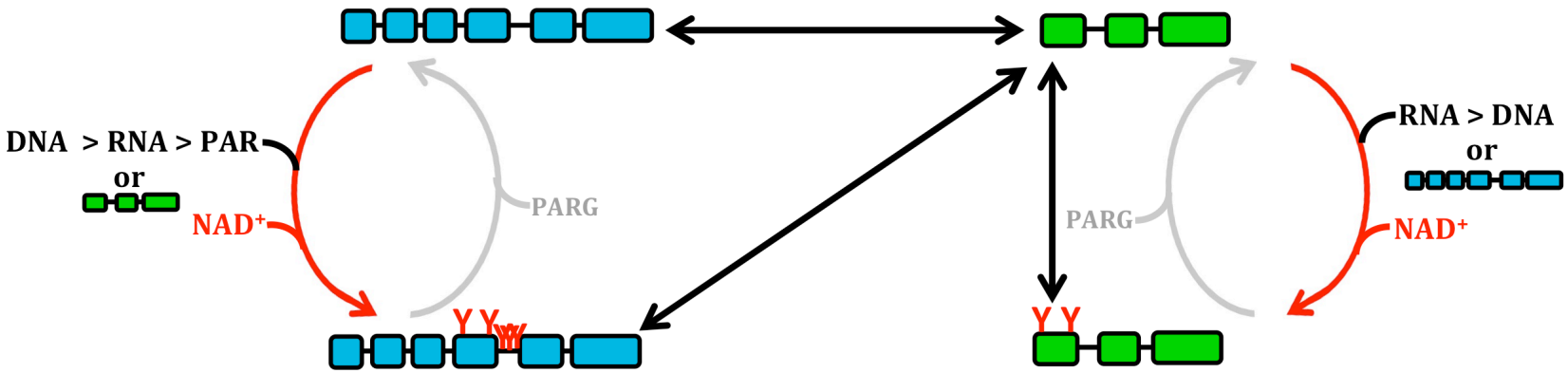

Figure 13: Signaling cascade of PARP-1 and PARP-2 during DNA damage and gene transcription
A. Model for PAR-dependent signaling cascade of PARP-1 and PARP-2 in response to DNA damage and transcription. Red arrows indicate enzymatic reactions and black double head arrows indicate a binding event. Individually, PARP-1 automodifies in the presence of allosteric activators (most prominently, DNA) and NAD^+. The initial automodification can trigger the activation of neighboring PARP-1 moles, propagating a PAR-mediated signal. PARP-2 automodifies in the presence of RNA (ds or ss) and NAD^+. The slower kinetics of PARP-2 activation may stabilize PARP and PAR function at sites of DNA damage and transcription. During complex formation, unmodified PARP-1 and PARP-2 bind to form a heterodimer capable of trans-activation when NAD^+ is present, although it unknown which protein becomes PARylated. Unmodified PARP-2 is also capable of forming dimers with automodified PARP-1 and PARP-2. The function of the three dimeric complexes is unclear. Once repair or transcriptional processes are complete, PARG (gray) will digest PAR allowing PARP-1 and PARP-2 to return to their native states.

SUMMARY & FUTURE DIRECTIONS

PARP-1 is involved in chromatin dynamics and gene expression in both an enzyme activity dependent and independent way. In its inactive form, PARP-1 condenses chromatin and acts as a chromatin architectural protein; when active, PARP-1 is able to function as both a scaffolding protein to recruit transcription complexes as well as a histone chaperone capable of nucleosome assembly. Lesser studied in terms of chromatin dynamics and gene expression, the interaction of PARP-2 in a chromatin context is unclear.

Here, I have quantified both the enzymatic activities and binding affinities for PARP-1 and PARP-2 in the presence of various nuclear components from nucleic acids to nucleosomes. Overall, the data presented herein points towards three primary findings. First, PARP-1 is enzymatically activated by its enzymatic product, PAR. This finding suggests a mechanism for PARP-1 spreading at sites of active gene expression, a phenomenon observed, for example, on heat shock genes. Second, PARP-2 is predominately activated by RNA, both single and double stranded, to similar levels as exhibited by PARP-1. Thus, while PARP-2 is an overall less efficient enzyme due to slight structural differences in the active site, stimulation by RNA can overcome this deficit. PARP-2 interacts only weakly with both native and damaged chromatin implicating PARP-1 as the primary chromatin interacting PARP in the nucleus. The weak interaction exhibited by PARP-2 is most likely due to the non-canonical N-terminal domain. Third and lastly, PARP-1 and PARP-2 form a heterodimer capable of trans-activation. Complex formation suggests PARP-1 and PARP-2

may function in a PAR-mediated signaling and recruitment cascade during DNA damage repair and active gene expression.

Ideally, all of the results presented here should be confirmed with *in vivo* studies, particularly the possibility of a PAR mediated spreading mechanism of PARP-1 at DNA damage and active transcription sites. Moreover, while PARP-1 prefers DNA as its activator, PARP-2 is strongly activated by single stranded RNA. This could implicate the prevalence of PARP-2 on the RNA processing side of transcription and should be explored *in vivo*. Further *in vitro* studies should be conducted to identify the structural basis of how DNA and RNA bind PARP-2. It has been suggested that DNA binds the WGR domain of PARP-2 (13) rather than the SAP DNA binding domain, the location of RNA binding (57). This evidence suggests the N-terminal domain of PARP-2 dispensable for DNA-dependent functions, but becomes required for functions mediated by an interaction with RNA; however, further biophysical and structural studies need to be done.

In a chromatin context, due to the involvement of PARP-1 in both inactive and active gene expression paralleled with its function as a histone chaperone, the interaction of PARP-1 with histone variants, notably H2A.Z and H3.3, should be explored. Lastly, we are working towards crystallizing PARP-1 in complex with the linker ended mononucleosome to provide the first structural insight into how PARP-1 binds DNA damaged chromatin.

The relationship of PARP-2 with chromatin is unique compared to PARP-1. Overall, PARP-2 exhibits weaker affinities for nucleic acids and nucleosomes; however, these affinities are

still low nanomolar and thus, relatively strong. The exception here is with PARP-2 and NLE-trinucleosomes exhibiting a high nanomolar affinity. These affinities may be strengthened if the DNA linker ends on the nucleosome are lengthened from 7 and 11 base pairs, as in the 165 mononucleosome. Overall, the interaction of PARP-2 with nucleosomes is still elusive and requires further study. Small angle X-ray scattering (SAXS), hydrogen-deuterium exchange coupled with mass spectrometry (HDX), and composition gradient small angle light scattering (CG-MALS) techniques could provide more conclusive evidence than what was seen with Job plots and AUC. Further exploring the interaction of PARP-2 with chromatin could provide more specificity to this protein and help us understand its distinct function within the nucleus.

Similar to PARP-1, due to the gain in histone affinity upon PARP-2 automodification suggest PARP-2 may also function as a histone chaperone when active. To confirm this, nucleosome assembly assay must be performed and confirmed with *in vivo* studies. However, since the possible histone chaperone activity of PARP-2 is dependent on enzymatic activity, PARP-2 will likely have drastically slow nucleosome assembly kinetics and may serve different functions (i.e. removing excess histones from reassembled nucleosomes or correcting improper nucleosome assembly, for example).

The interaction of PARP-1 and PARP-2 has been speculated in a few biochemical studies and evidence has been provided by pull down experiments (62, 88). Here, I show the ability of PARP-1 and PARP-2 to heterodimerize. The affinity of PARP-2 for PARP-1 increases 2-fold if the DNA binding N-terminal half of PARP-1 is removed. This finding indicates that

either the conformation of full length PARP-1 or the N-terminal domain has inhibitory properties. Strikingly, full length PARP-1 and PARP-2 affinity increases 2-fold when PARP-1 is automodified in the presence of DNA and NAD^+. The increase in affinity could be due to automodification inducing conformational changes in PARP-1 yielding a more open structure, but this needs to be explored further.

Lastly, in addition to forming a functional complex, PARP-1 and PARP-2 have the ability to trans-activate one another. PARP-2 activation of PARP-1 is not very significant, only 16% of DNA-dependent activation, but PARP-1 activation of PARP-2 is significant, 62% of DNA-dependent activation. Recruitment of PARP-2 is longer-lived and more stable at DNA damage sites compared to PARP-1, a very transient activity; thus trans-activity could indicate a mechanism for producing more stable PARylation at sites of DNA damage and gene expression. Additionally, PARP-2 has been suggested to function in post-translational modifications aside from PARylation, namely acetylation. The binding of PARP-2 to PARylated PARP-1 and PARP-2, in addition to unmodified PARP-1, could suggest a potential mechanism to recruit unmodified PARP-2 to sites of repair and expression allowing acetyltransferases to acetylate PARP-2. Nevertheless, the *in vivo* relevance and function of a trans-activating heterodimer remains obscure and unknown.

Future studies should include the identification of the PARP-1 and PARP-2 binding interface. Identifying the exact residues involved in binding could be determined by truncating PARP-2 into a N and C terminal halves for FRET experiments as well as hydrogen-deuterium exchange coupled with mass spectrometry (HDX-MS) experiments.

Additionally, complex formation could be confirmed *in vivo* with localization studies and possibly, fluorescent microscopy. Lastly, the functional implications of this complex need to be further explored to identify specific roles of the complex versus the individual functions of PARP-1 and PARP-2.

REFERENCES

1. Chambon P, Weill JD, & Mandel P (1963) Nicotinamide Mononucleotide Activation of a New DNA-Dependent Polyadenylic Acid Synthesizing Nuclear Enzyme. *Biochem and Biophys Res Comm* 11(1):39-43.
2. Ruf A, Rolli V, de Murcia G, & Schulz GE (1998) The Mechanism of the Elongation and Branching Reaction of Poly(ADP-ribose) Polymerase as Derived From Crystal Structures and Mutagenesis. *J Mol Biol* 278:57-65.
3. Luo X & Kraus WL (2012) On PAR with PARP: cellular stress signaling through poly(ADP-ribose) and PARP-1. *Genes Dev* 26(5):417-432.
4. Hottiger MO, Hassa PO, Luscher B, Schuler H, & Koch-Nolte F (2010) Toward a unified nomenclature for mammalian ADP-ribosyltransferases. *Trends in biochemical sciences* 35(4):208-219.
5. Ryu KW, Kim DS, & Kraus WL (2015) New Facets in the Regulation of Gene Expression by ADP-Ribosylation and Poly(ADP-ribose) Polymerases. *Chemical reviews* 115(6):2453-2481.
6. Kraus WL & Lis JT (2003) PARP Goes Transcription. *Cell* 113(6):677-683.
7. Clark NJ, Kramer M, Muthurajan UM, & Luger K (2012) Alternative modes of binding of poly(ADP-ribose) polymerase 1 to free DNA and nucleosomes. *The Journal of biological chemistry* 287(39):32430-32439.
8. Langelier MF, Planck JL, Roy S, & Pascal JM (2012) Structural basis for DNA damage-dependent poly(ADP-ribosyl)ation by human PARP-1. *Science* 336(6082):728-732.
9. Alano CC*, et al.* (2010) NAD+ depletion is necessary and sufficient for poly(ADP-ribose) polymerase-1-mediated neuronal death. *The Journal of neuroscience : the official journal of the Society for Neuroscience* 30(8):2967-2978.
10. Ko HL & Ren EC (2012) Functional Aspects of PARP1 in DNA Repair and Transcription. *Biomolecules* 2(4):524-548.
11. Altmeyer M, Messner S, Hassa PO, Fey M, & Hottiger MO (2009) Molecular mechanism of poly(ADP-ribosyl)ation by PARP1 and identification of lysine residues as ADP-ribose acceptor sites. *Nuc Acids Res* 37(11):3723-3738.
12. Ruf A, Menissier-de Murcia J, de Murcia G, & Schulz GE (1996) Structure of the catalytic fragment of poly(ADP-ribose) polymerase from chicken. *PNAS* 93:7481-7485.
13. Langelier MF, Riccio AA, & Pascal JM (2014) PARP-2 and PARP-3 are selectively activated by 5' phosphorylated DNA breaks through an allosteric regulatory mechanism shared with PARP-1. *Nuc Acids Res* 42(12):7762-7775.
14. Oliver AW, Ame J, Roe SM, Good V, & de Murcia G (2004) Crystal structure of the catalytic fragment of murine poly(ADP-ribose) polymerase-2. *Nuc Acids Res* 32(2):456-464.
15. Langelier MF, Servent KM, Rogers EE, & Pascal JM (2008) A third zinc-binding domain of human poly(ADP-ribose) polymerase-1 coordinates DNA-dependent enzyme activation. *The Journal of biological chemistry* 283(7):4105-4114.
16. Langelier MF, Ruhl DD, Planck JL, Kraus WL, & Pascal JM (2010) The Zn3 domain of human poly(ADP-ribose) polymerase-1 (PARP-1) functions in both DNA-dependent

poly(ADP-ribose) synthesis activity and chromatin compaction. *The Journal of biological chemistry* 285(24):18877-18887.
17. Shieh WM*, et al.* (1998) Poly(ADP-ribose) Polymerase Null Mouse Cells Synthesize ADP-ribose Polymers. *The Journal of biological chemistry* 273(46):30069-30072.
18. Ame JC*, et al.* (1999) PARP-2, A Novel Mammalian DNA Damage-dependent Poly(ADP-ribose) Polymerase. *The Journal of biological chemistry* 274(25):17860-17868.
19. Szanto M*, et al.* (2012) Poly(ADP-ribose) polymerase-2: emerging transcriptional roles of a DNA-repair protein. *Cellular and molecular life sciences : CMLS* 69(24):4079-4092.
20. Aravind L & Koonin EV (2000) SAP – a putative DNA-binding motif involved in chromosomal organization. *Trends in biochemical sciences* 25(3):112-114.
21. Haenni SS*, et al.* (2008) Identification of lysines 36 and 37 of PARP-2 as targets for acetylation and auto-ADP-ribosylation. *Int J Biochem Cell Biol* 40(10):2274-2283.
22. Schreiber V*, et al.* (2006) PARP-2: Structure-Function Relationship. *Mol Biol Intell*:13-31.
23. Luger K, Mader AW, Richmond RK, Sargent DF, & Richmond TJ (1997) Crystal structure of the nucleosome core particle at 2.8A resolution. *Nature* 389:251-260.
24. Knezetic JA & Luse DS (1986) The Presence of Nucleosomes on a DNA Template Prevents Initiation by RNA Polymerase II In Vitro. *Cell* 45:95-104.
25. Burgess RJ & Zhang Z (2013) Histone chaperones in nucleosome assembly and human disease. *Nature structural & molecular biology* 20(1):14-22.
26. De Koning L, Corpet A, Haber JE, & Almouzni G (2007) Histone chaperones: an escort network regulating histone traffic. *Nature structural & molecular biology* 14(11):997-1007.
27. Eitoku M, Sato L, Senda T, & Horikoshi M (2008) Histone chaperones: 30 years from isolation to elucidation of the mechanisms of nucleosome assembly and disassembly. *Cellular and molecular life sciences : CMLS* 65(3):414-444.
28. Hansen JC (2002) Conformational dynamics of the chromatin fiber in solution: determinants, mechanisms, and functions. *Annual review of biophysics and biomolecular structure* 31:361-392.
29. Muthurajan UM*, et al.* (2014) Automodification switches PARP-1 function from chromatin architectural protein to histone chaperone. *PNAS* 111(35):12752-12757.
30. Petesch SJ & Lis JT (2012) Overcoming the nucleosome barrier during transcript elongation. *Trends Genet* 28(6):285-294.
31. Teves SS, Weber CM, & Henikoff S (2014) Transcribing through the nucleosome. *Trends in biochemical sciences* 39(12):577-586.
32. Wacker DA*, et al.* (2007) The DNA binding and catalytic domains of poly(ADP-ribose) polymerase 1 cooperate in the regulation of chromatin structure and transcription. *Mol Cell Biol* 27(21):7475-7485.
33. McBryant SJ, Adams VH, & Hansen JC (2006) Chromatin architectural proteins. *Chromosome research : an international journal on the molecular, supramolecular and evolutionary aspects of chromosome biology* 14(1):39-51.
34. Kraus WL & Hottiger MO (2013) PARP-1 and gene regulation: progress and puzzles. *Molecular aspects of medicine* 34(6):1109-1123.

35. Kim MY, Mauro S, Gevry N, Lis JT, & Kraus WL (2004) NAD+-dependent modulation of chromatin structure and transcription by nucleosome binding properties of PARP-1. *Cell* 119(6):803-814.
36. Krishnakumar R*, et al.* (2008) Reciprocal Binding of PARP-1 and Histone H1 at Promoters Specifies Transcriptional Outcomes. *Science* 319:819-821.
37. Yelamos J, Schreiber V, & Dantzer F (2008) Toward specific functions of poly(ADP-ribose) polymerase-2. *Trends in molecular medicine* 14(4):169-178.
38. Yelamos J, Farres J, Liacuna L, Ampurdanes C, & Martin-Caballero J (2011) PARP-1 and PARP-2: New players in tumour development. *Am J Cancer Res* 1(3):328-346.
39. Saxena A*, et al.* (2002) Poly(ADP-ribose) polymerase 2 localizes to mammalian active centromeres and interacts with PARP-1, Cenpa, Cenpb and Bub3, but not Cenpc. *Human Mol Gen* 11(19):2319-2329.
40. Dantzer F*, et al.* (2004) Functional Interaction between Poly(ADP-Ribose) Polymerase 2 (PARP-2) and TRF2: PARP Activity Negatively Regulates TRF2. *Mol Cell Biol* 24(4):1595-1607.
41. Beneke S*, et al.* (2008) Rapid regulation of telomere length is mediated by poly(ADP-ribose) polymerase-1. *Nuc Acids Res* 36(19):6309-6317.
42. Dantzer F*, et al.* (2006) Poly(ADP-ribose) polymerase-2 contributes to the fidelity of male meiosis I and spermiogenesis. *PNAS* 103(40):14854-14859.
43. Meyer-Ficca ML*, et al.* (2011) Poly(ADP-ribose) polymerases PARP1 and PARP2 modulate topoisomerase II beta (TOP2B) function during chromatin condensation in mouse spermiogenesis. *Biology of reproduction* 84(5):900-909.
44. Mathis G & Althaus FR (1987) release of core DNA from nucleosomal core particles following (ADP-ribose)n-modification in vitro. *Biochem Biophys Res Comm* 143:1049-1054.
45. Tulin A & Spradling A (2003) Chromatin loosening by poly(ADP)-ribose polymerase (PARP) at Drosophila puff loci. *Science* 299(5606):560-562.
46. Petesch SJ & Lis JT (2012) Activator-induced spread of poly(ADP-ribose) polymerase promotes nucleosome loss at Hsp70. *Molecular cell* 45(1):64-74.
47. Petesch SJ & Lis JT (2008) Rapid, transcription-independent loss of nucleosomes over a large chromatin domain at Hsp70 loci. *Cell* 134(1):74-84.
48. D'Amours D, Desnoyers S, D'Silva I, & Poirier G (1999) Poly(ADP-ribosyl)ation reactions in the regulation of nuclear functions. *The Journal of biological chemistry* 342:249-258.
49. Thomas CJ*, et al.* (2014) Kinase-mediated changes in nucleosome conformation trigger chromatin decondensation via poly(ADP-ribosyl)ation. *Molecular cell* 53(5):831-842.
50. Jungmichel S*, et al.* (2013) Proteome-wide identification of poly(ADP-Ribosyl)ation targets in different genotoxic stress responses. *Molecular cell* 52(2):272-285.
51. Khoury-Haddad H*, et al.* (2014) PARP1-dependent recruitment of KDM4D histone demethylase to DNA damage sites promotes double-strand break repair. *PNAS* 111(7):728-737.
52. Hassa PO & Hottiger MO (2002) The functional role of poly(ADP-ribose)polymerase 1 as novel coactivator of NF-kB in inflammatory disorders. *Cell Mol. Life Sci* 59:1534-1553.
53. Isabelle M*, et al.* (2010) Investigation of PARP-1, PARP-2, and PARG interactomes by affinity-purification mass spectrometry. *Proteome Sci* 8:22.

54. Ji Y & Tulin AV (2009) Poly(ADP-ribosyl)ation of heterogeneous nuclear ribonucleoproteins modulates splicing. *Nuc Acids Res* 37(11):3501-3513.
55. Bai P*, et al.* (2011) PARP-2 regulates SIRT1 expression and whole-body energy expenditure. *Cell metabolism* 13(4):450-460.
56. Liang YC, Hsu CY, Yao YL, & Yang WM (2013) PARP-2 regulates cell cycle-related genes through histone deacetylation and methylation independently of poly(ADP-ribosyl)ation. *Biochemical and biophysical research communications* 431(1):58-64.
57. Leger K, Bar D, Savic N, Santoro R, & Hottiger MO (2014) ARTD2 activity is stimulated by RNA. *Nuc Acids Res* 42(8):5072-5082.
58. Potaman VN, Shlyakhtenko LS, Oussatcheva EA, Lyubchenko YL, & Soldatenkov VA (2005) Specific binding of poly(ADP-ribose) polymerase-1 to cruciform hairpins. *J Mol Biol* 348(3):609-615.
59. Ame JC, Spenlehauer C, & de Murcia G (2004) The PARP superfamily. *Bioessays* 26(8):882-893.
60. Prasad R*, et al.* (2014) Suicidal cross-linking of PARP-1 to AP site intermediates in cells undergoing base excision repair. *Nucleic acids research* 42(10):6337-6351.
61. Swindall AF, Stanley JA, & Yang ES (2013) PARP-1: Friend or Foe of DNA Damage and Repair in Tumorigenesis? *Cancers* 5(3):943-958.
62. Schreiber V*, et al.* (2002) Poly(ADP-ribose) polymerase-2 (PARP-2) is required for efficient base excision DNA repair in association with PARP-1 and XRCC1. *The Journal of biological chemistry* 277(25):23028-23036.
63. Kutuzov MM*, et al.* (2013) Interaction of PARP-2 with DNA structures mimicking DNA repair intermediates and consequences on activity of base excision repair proteins. *Biochimie* 95(6):1208-1215.
64. Wang M*, et al.* (2006) PARP-1 and Ku compete for repair of DNA double strand breaks by distinct NHEJ pathways. *Nucleic acids research* 34(21):6170-6182.
65. Audebert M, Salles B, & Calsou P (2004) Involvement of poly(ADP-ribose) polymerase-1 and XRCC1/DNA ligase III in an alternative route for DNA double-strand breaks rejoining. *The Journal of biological chemistry* 279(53):55117-55126.
66. Audebert M, Salles B, Weinfeld M, & Calsou P (2006) Involvement of polynucleotide kinase in a poly(ADP-ribose) polymerase-1-dependent DNA double-strand breaks rejoining pathway. *J Mol Biol* 356(2):257-265.
67. Schultz T, Lopez E, Saleh-Gohari N, & Helleday T (2003) Poly(ADP-ribose) polymerase (PARP-1) has a controlling role in homologous recombination. *Nuc Acids Res* 31(17):4959-4964.
68. Nguyen D*, et al.* (2011) Poly(ADP-ribose) polymerase inhibition enhances p53-dependent and -independent DNA damage responses induced by DNA damaging agent. *Cell cycle* 10(23):4074-4082.
69. Orlando G, Khoronenkova SV, Dianova II, Parsons JL, & Diano GL (2014) ARF induction in response to DNA strand breaks is regulated by PARP1. *Nuc Acids Res* 42(4):2320-2329.
70. Huber A, Bai P, de Murcia JM, & de Murcia G (2004) PARP-1, PARP-2 and ATM in the DNA damage response: functional synergy in mouse development. *DNA repair* 3(8-9):1103-1108.
71. Soldani C & Scovassi AI (2002) Poly(ADP-ribose) polymerase-1 cleavage during apoptosis: An update. *Apoptosis* 7(4):321-328.

72. Chaitanya GV, Steven AJ, & Babu PP (2010) PARP-1 cleavage fragments: signatures of cell-death proteases in neurodegeneration. *Cell communication and signaling : CCS* 8:31.
73. Gobeil S, Boucher CC, Nadeau D, & Poirier GG (2001) Characterization of the necrotic cleavage of poly(ADP-ribose) polymerase (PARP-1): implication of lysosomal proteases. *Cell Death Differ* 8(6):588-594.
74. Yu SW*, et al.* (2006) Apoptosis-inducing factor mediates poly(ADP-ribose) (PAR) polymer-induced cell death. *PNAS* 103(48):18314-18319.
75. Benchoua A*, et al.* (2002) Active caspase-8 translocates into the nucleus of apoptotic cells to inactivate poly(ADP-ribose) polymerase-2. *The Journal of biological chemistry* 277(37):34217-34222.
76. Beneke S, Scherr AL, Ponath V, Popp O, & Burkle A (2010) Enzyme characteristics of recombinant poly(ADP-ribose) polymerases-1 of rat and human origin mirror the correlation between cellular poly(ADP-ribosyl)ation capacity and species-specific life span. *Mech Ageing Dev* 131(5):366-369.
77. Michaelis L, Menten ML, Johnson KA, & Goody RS (2011) The original Michaelis constant: translation of the 1913 Michaelis-Menten paper. *Biochemistry* 50(39):8264-8269.
78. Langelier MF, Planck JL, Servent KM, & Pascal JM (2011) Purification of human PARP-1 and PARP-1 domains from Escherichia coli for structural and biochemical analysis. *Methods Mol Biol* 780:209-226.
79. Carter-O'Connel I, Jin H, Morgan RK, David LL, & Cohen MS (2014) Engineering the substrate specificity of ADP-ribosyltransferases for identifying direct protein targets. *J Am Chem Soc* 136(14):5201-5204.
80. Hieb AR, D'Arcy S, Kramer MA, White AE, & Luger K (2012) Fluorescence strategies for high-throughput quantification of protein interactions. *Nuc Acids Res* 40(5):e33.
81. Dyer PN*, et al.* (2004) Reconstitution of Nucleosome Core Particles from Recombinant Histones and DNA. *Methods Enzymol* 375:23-44.
82. Winkler DD, Muthurajan UM, Hieb AR, & Luger K (2011) Histone chaperone FACT coordinates nucleosome interaction through multiple synergistic binding events. *The Journal of biological chemistry* 286(48):41883-41892.
83. Olson EJ & Buhlmann P (2011) Getting more out of a Job plot: determination of reactant to product stoichiometry in cases of displacement reactions and n:n complex formation. *The Journal of organic chemistry* 76(20):8406-8412.
84. Krishnakumar R & Kraus WL (2010) The PARP side of the nucleus: molecular actions, physiological outcomes, and clinical targets. *Molecular cell* 39(1):8-24.
85. Yelamos J, Farres J, Llacuna L, Ampurdanes C, & Martin-Caballero J (2011) PARP1 and PARP2: New players in tumour development. *Am J Cancer Res* 1(3):328-346.
86. Pinnola A, Naumova N, Shah M, & Tulin AV (2007) Nucleosomal core histones mediate dynamic regulation of poly(ADP-ribose) polymerase 1 protein binding to chromatin and induction of its enzymatic activity. *The Journal of biological chemistry* 282(44):32511-32519.
87. El-Sagheer AH*, et al.* (2008) A very stable cyclic DNA miniduplex with just two base pairs. *Chembiochem* 9(1):50-52.
88. Mennissier de Murcia J*, et al.* (2003) Functional interaction between PARP-1 and PARP-2 in chromosome stability and embryonic development in mouse. *EMBO* 22(9):2255-2263.

89. Diefenbach J & Burkle A (2005) Introduction to poly(ADP-ribose) metabolism. *Cellular and molecular life sciences : CMLS* 62(7-8):721-730.
90. Kraus WL (2008) Transcriptional control by PARP-1: chromatin modulation, enhancer-binding, coregulation, and insulation. *Current opinion in cell biology* 20(3):294-302.

APPENDIX I

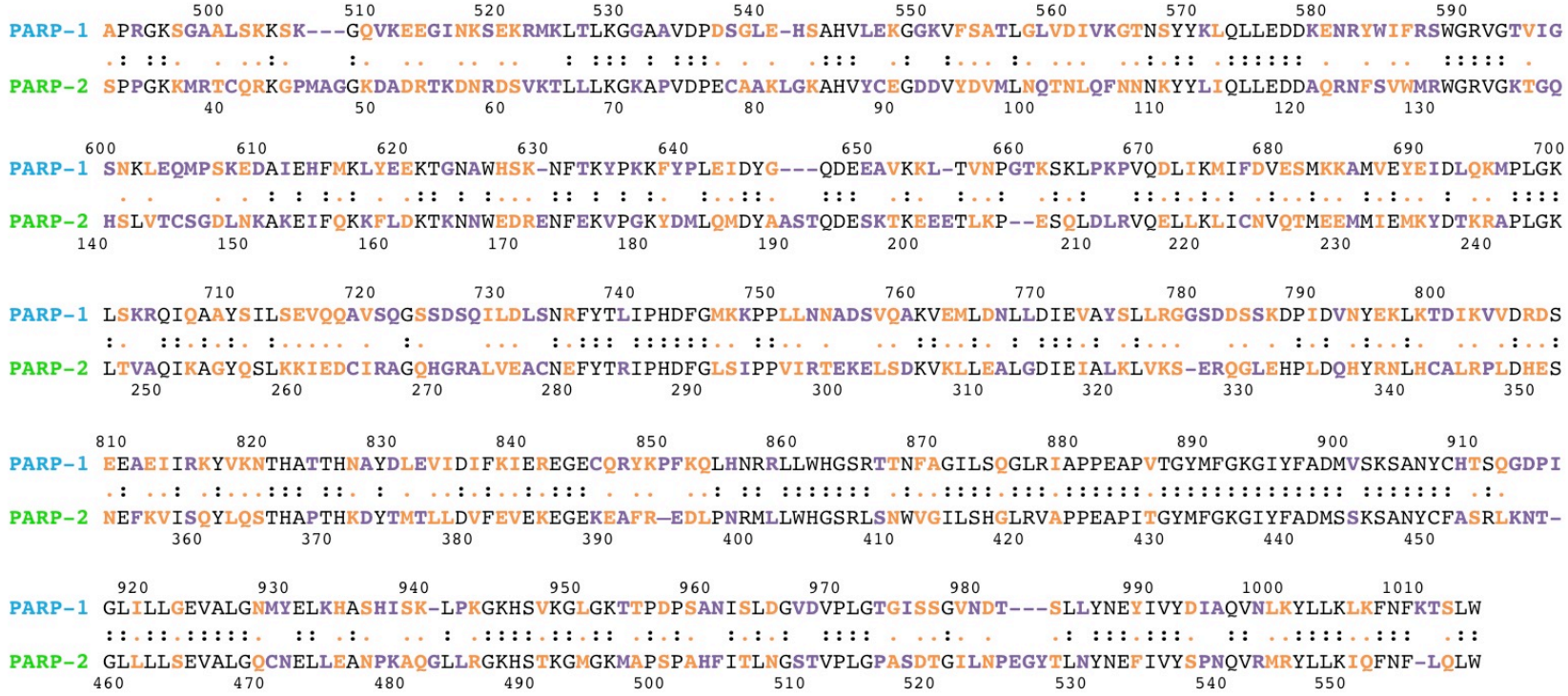

Key:
Conserved (:)
Similar charge and shape (.)
No match

Supplementary Figure 14: Sequence alignment of PARP-1 and PARP-2.
Sequence alignment for human PARP-1 and mouse PARP-2 by the LALIGN server. PARP-1 and PARP-2 have a 40.3% identity and 70.3% similarity.

A.

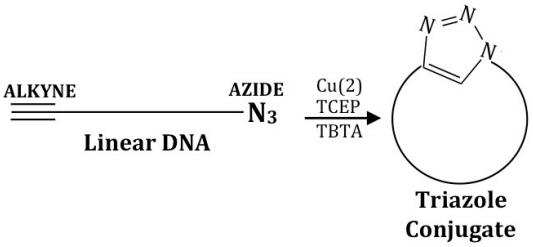

B.

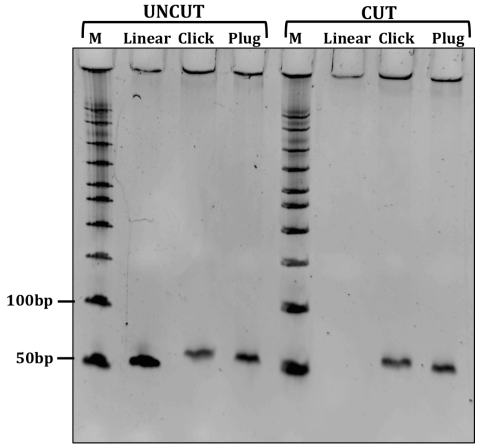

C.

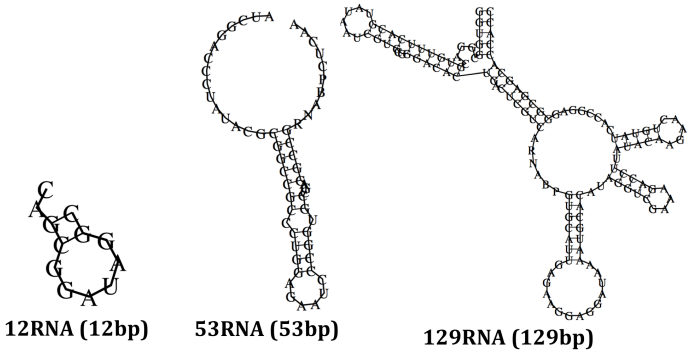

Supplementary Figure 15: Nucleic acid reagents used in the enzyme assay

- **A.** Schematic of the click chemistry reaction. In the presence of copper (II), an azide and alkyne will join in a 1,2,3-triazole linkage.
- **B.** Quality control of click chemistry reaction in 3A. M: Molecular weight marker; Linear: 53bp DNA with no modifications; Click: Circularized DNA; Plug: Linear 53bp DNA with attached azide and alkyne groups. Clicked and plugged DNA have slightly slower migration compared to linear DNA due to difference in shape. The 5' exonuclease digests the linear DNA but not the protected clicked or plugged DNA indicative of successful triazole linkage formation in the click reaction.
- **C.** RNA fold predictions of the single stranded RNAs used in the enzyme assay and FRET experiments. Predictions from RNAfold web server.

Calculating Kinetic Parameters for Enzyme Assay

Raw Velocity (pMol/min)

$$\frac{\text{Fluorescent Signal}}{\text{Slope of Standard}} \rightarrow \textbf{pMol NAD+/µL} \times \frac{\text{Volume (uL)}}{} \times \frac{}{\text{1m}} \rightarrow \textbf{pMol NAD}^{+}\textbf{/min}$$

V_{max} (µmol/min/mg)

$$\frac{\text{Raw Velocity (pMol/min)}}{\text{mg PARP1 in sample}} \times \frac{\text{1µMol}}{1\text{x}10^{6}\text{ pMol}} \rightarrow \textbf{µMol NAD}^{+}\textbf{/min/mg}$$

K_m (µM)

Straight from Graphpad

---

k_{cat} (s^{-1})

$$\frac{V_{max}\text{ (µMol/min/mg)}}{\text{60s}} \times \frac{\text{1000mg}}{\text{1g}} \times \frac{\text{1 mole}}{1\text{x}10^{6}\text{ µMol}} \times \frac{\text{MW (g)}}{\text{1 mole}} \rightarrow s^{-1}$$

---

k_{cat}/K_m ($s^{-1} M^{-1}$)

$$\frac{K_m\text{ (µM)}}{1\text{x}10^{6}\text{ µM}} \rightarrow \textbf{K}_m\textbf{ (M)}$$

$$\frac{k_{cat}\ (s^{-1})}{K_m\text{ (M)}} \rightarrow s^{-1}\,M^{-1}$$

Supplementary Figure 16: Calculating kinetic parameters for enzyme assay

A.

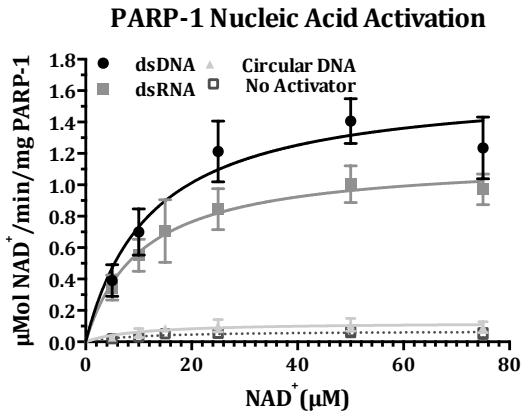
PARP-1 Nucleic Acid Activation
dsDNA
dsRNA
Circular DNA
No Activator
µMol NAD+/min/mg PARP-1
NAD+(µM)

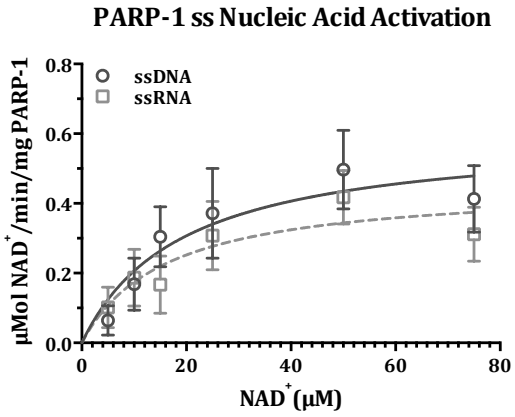
PARP-1 ss Nucleic Acid Activation
ssDNA
ssRNA
µMol NAD+/min/mg PARP-1
NAD+(µM)

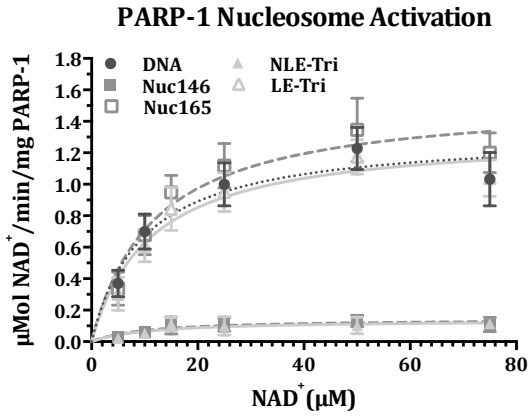
PARP-1 Nucleosome Activation
DNA
Nuc146
Nuc165
NLE-Tri
LE-Tri
µMol NAD+/min/mg PARP-1
NAD+(µM)

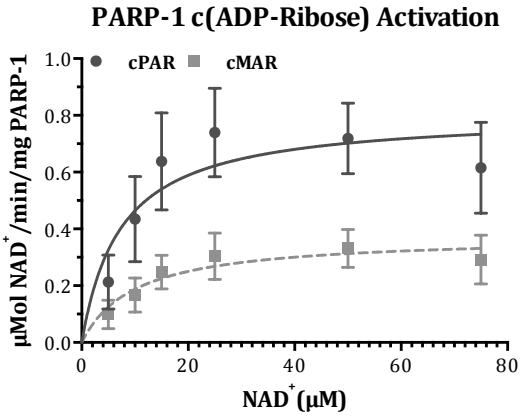
PARP-1 c(ADP-Ribose) Activation
cPAR
cMAR
µMol NAD+/min/mg PARP-1
NAD+(µM)

B.

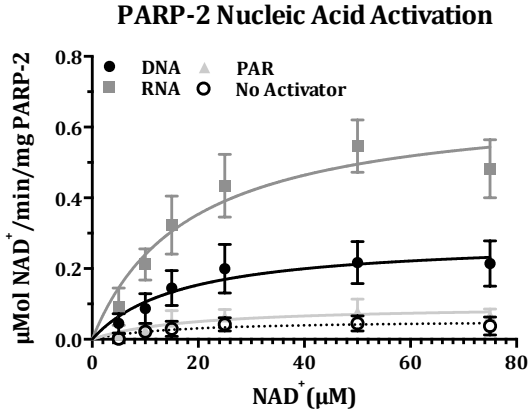
PARP-2 Nucleic Acid Activation
DNA
RNA
PAR
No Activator
µMol NAD+/min/mg PARP-2
NAD+(µM)

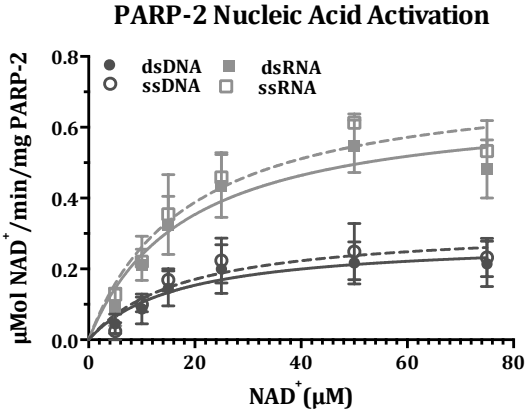
PARP-2 Nucleic Acid Activation
dsDNA
ssDNA
dsRNA
ssRNA
µMol NAD+/min/mg PARP-2
NAD+(µM)

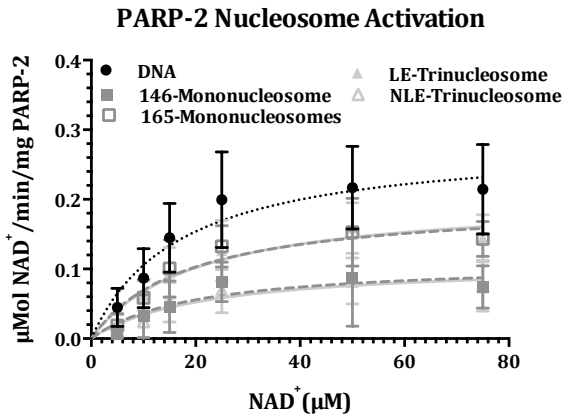

Supplementary Figure 17: Michaelis-Menten Curves

Raw data from Table 1.

- **A.** PARP-1 Michaelis-Menten curves for activators reported here.
- **B.** PARP-2 Michaelis-Menten curves for activators reported here.

A.

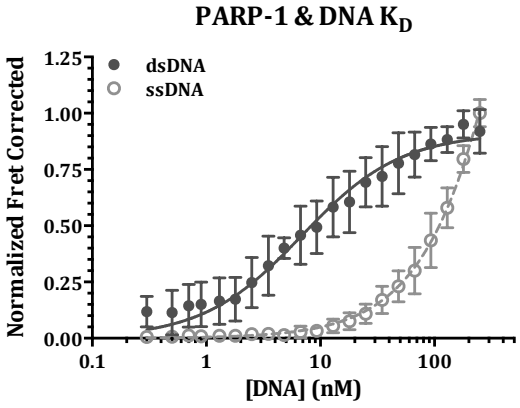
PARP-1 & DNA K_D
dsDNA
ssDNA
Normalized Fret Corrected
[DNA] (nM)

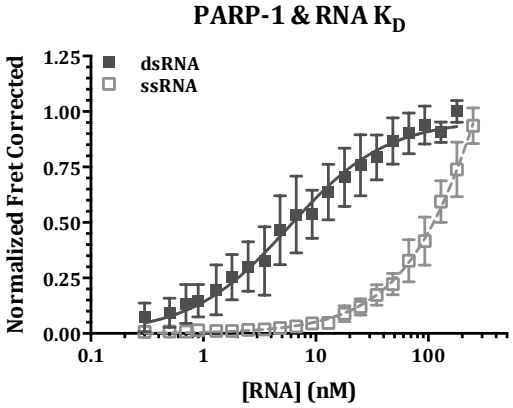
PARP-1 & RNA K_D
dsRNA
ssRNA
Normalized Fret Corrected
[RNA] (nM)

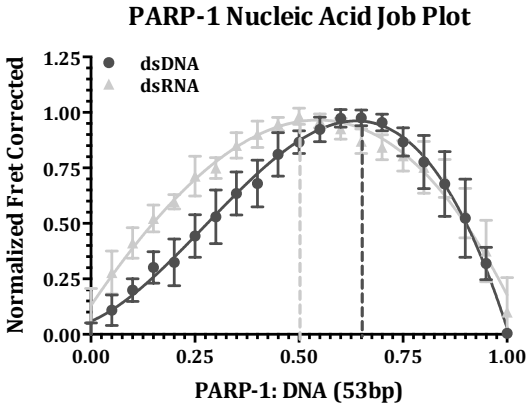
PARP-1 Nucleic Acid Job Plot
dsDNA
dsRNA
Normalized Fret Corrected
PARP-1: DNA (53bp)

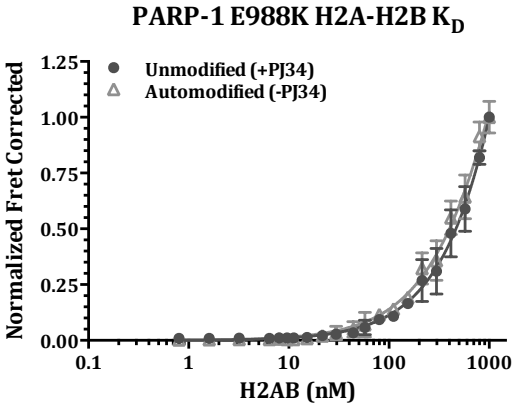
PARP-1 E988K H2A-H2B K_D
Unmodified (+PJ34)
Automodified (-PJ34)
Normalized Fret Corrected
H2AB (nM)

B.

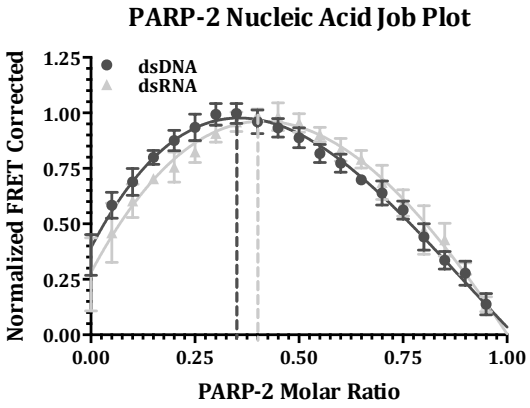
PARP-2 Nucleic Acid Job Plot
dsDNA
dsRNA
Normalized FRET Corrected
PARP-2 Molar Ratio

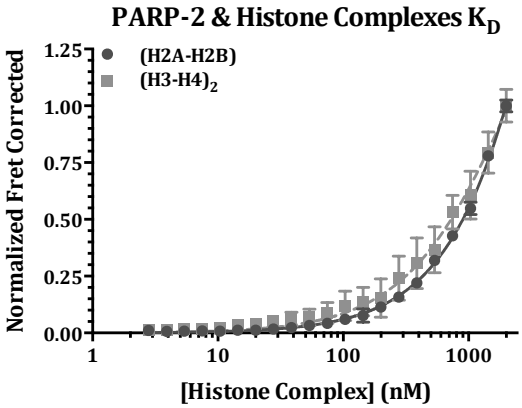
PARP-2 & Histone Complexes K_D
(H2A-H2B)
$(H3-H4)_2$
Normalized Fret Corrected
[Histone Complex] (nM)

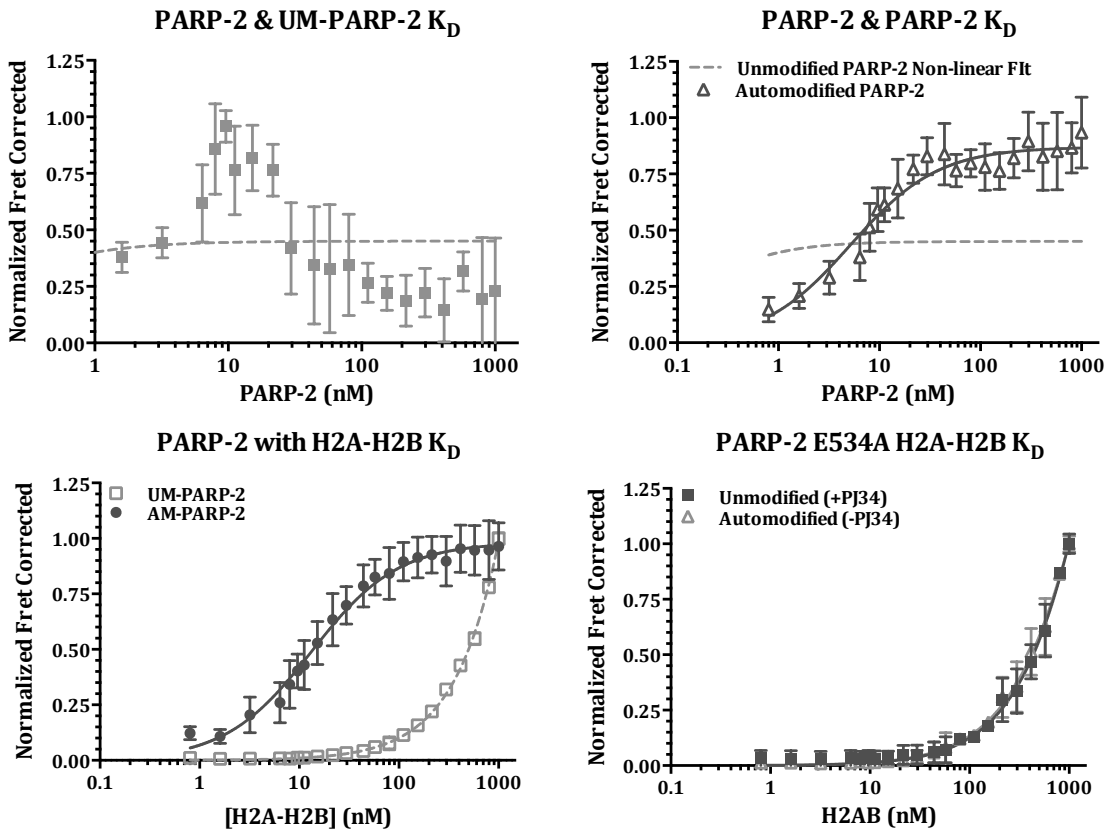

Supplementary Figure 18: HIFI-FRET Binding Curves

Raw data from Table 2 and 3.

A. PARP-1 binding curves for activators reported here.

B. PARP-2 binding curves for activators reported here.

APPENDIX II

Supplementary Table 4: Comparison of Sf9 insect cells and *E. coli* expressed PARP-1 activity and affinity.

Activator & Ligand	Sf9 Insect Cells		*E. coli*	
	$K_D^{(app)}$ *(nM)*	V_{max} *(µmol/min/mg)*	$K_D^{(app)}$ *(nM)*	V_{max} *(µmol/min/mg)*
Basal Activity		0.0094		0.076±0.05
Nucleic Acids				
Circular DNA		0.188		0.163±0.03
dsDNA	27.8 ± 5.6	0.5411	6.8±0.4	1.57±0.34
Histones				
H2A-H2B-	>500[2]		>500	0.127±0.02
$(H3\text{-}H4)_2$	>500[2]		>500	0.116±0.01
Chromatin				
Nuc146	>500[1]	0.0823	>500	0.145±0.01
Nuc165	2.2±1.5[1]	0.7864*	2.5±0.6	1.76±0.22
NLE-Tri	4.8±2.1[2]		12.7±0.6	0.14±0.02
LE-Tri	12.7±6.7[2]			1.70±0.11

[1] Clark et al, 2012. JBC [2] Muthurajan et al, 2014. PNAS.

* Symmetric Nuc207

Supplementary Table 5: Fold stimulation of PARP-1 and PARP-2 enzymatic activation

Allosteric Activator	PARP-1		PARP-2		Fold Difference	
	Fold V_{max} *(Activator/Basal)*	% Relative to DNA	Fold V_{max} *(Activator/Basal)*	% Relative to DNA	V_{max} *(PARP-1/PARP-2)*	k_{cat}/K_M *(PARP-1/PARP-2)*
Basal Activity	1.0	4.8	1.0	15.4	1.4	5.4
Nucleic Acids						
Circular DNA	2.1	10.4	1.0	14.9	3.1	17.3
dsDNA (53bp)	20.7	100.0	6.5	100.0	4.4	20.0
ssDNA (53bp)	8.2	39.5	7.7	118.5	1.5	9.4
dsRNA (53bp)	13.4	65.0	12.9	199.7	1.4	6.5
ssRNA (53bp)	6.7	32.6	13.6	210.4	0.7	3.6
ssRNA (12bp)	7.0	33.9	14.4	221.9	1.5	3.4
ssRNA (129bp)	8.5	41.1	13.7	212.4	1.2	4.7
Histones						
(H2A-H2B)	1.5	8.1	2.2	34.0	1.0	5.6
$(H3\text{-}H4)_2$	1.5	7.4	2.5	37.9	0.9	5.6
Chromatin						
Nuc146	1.9	9.2	1.5	23.3	1.7	10.9
Nuc165	23.2	112.1	3.7	57.3	8.6	37.3
NLE Tri	1.8	8.9	1.0	18.3	2.2	11.8
LE-Tri	22.4	108.3	3.7	57.9	8.3	44.6
ADP-Ribose						
cMAR	4.9	23.9				
cPAR	9.4	45.7	0.9	14.0	14.4	104.1
AM-PARP-1 (5')	9.2	44.5				
AM-PARP-1 (120')	7.9	38.2				
AM-PARP-1 (ON')	5.0	24.1				
FL-PARP						
PARP-1/PARP-2	3.3	15.8	4.0	61.5	1.1	5.9

**Raw values taken from Table 1*

Supplementary Table 6: Fold difference in PARP-1 and PARP-2 K_D values

Binding Ligand	Fold Difference
	K_D^{app} *(PARP-2/PARP-1)*
Nucleic Acids	
dsDNA (53bp)	8.3
ssDNA (53bp)	1.0
dsRNA (53bp)	8.3
ssRNA (53bp)	1.0
Histones	
(H2A-H2B)	1.0
$(H3\text{-}H4)_2$	1.0
Chromatin	
Nuc146	1.0
Nuc165	42.2
NLE Tri	79.5